Available online at www.sciencedirect.com
SCIENCE DIRECT®
Coordination Chemistry Reviews 249 (2005) 2763–2786
COORDINATION CHEMISTRY REVIEWS
www.elsevier.com/locate/ccr

Review

Annual survey of organometallic metal cluster chemistry for the year 2003

Michael G. Richmond *

Department of Chemistry, University of North Texas, Denton, TX 76203, USA

Received 7 February 2005
Available online 28 March 2005

Contents

1. Dissertations 2763
2. Homometallic clusters 2764
   2.1. Group 6 clusters 2764
   2.2. Group 7 clusters 2764
   2.3. Group 8 clusters 2765
   2.4. Group 9 clusters 2773
   2.5. Group 10 clusters 2775
   2.6. Group 11 clusters 2776
3. Heterometallic clusters 2776
   3.1. Trinuclear clusters 2776
   3.2. Tetranuclear clusters 2779
   3.3. Pentanuclear clusters 2781
   3.4. Hexanuclear clusters 2781
   3.5. Higher nuclearity clusters 2783
   Appendix A 2783
   References 2783

Abstract

The synthetic, mechanistic, and structural chemistry of organometallic metal cluster compounds is reviewed for the year 2003.

Keywords: Organometallic cluster compounds; Polynuclear compounds

1. Dissertations

The reaction of *N*-phenyl-2,5-dimethyl-3,4-diphenylcyclopenta-2,4-dienimine with $Ru_3(CO)_{12}$ leads to cluster fragmentation and formation of *cis* and *trans* [{2,5-Me_2-3,4-Ph_2(η^5-C_4CNHPh)}Ru(CO)(μ-CO)]$_2$ [1]. $Os_3(CO)_{11}$(MeCN) has been allowed to react with 1,4-bis(ferrocenyl)butadiyne to give $Os_3(CO)_{10}(\mu,\eta^2$-FcC_4Fc) and $Os_3(CO)_{11}(\mu_3,\eta^4$-Fc$C_4$Fc). X-ray diffraction analyses have confirmed the coordination of one and both alkyne groups in these products, respectively. Whereas the redox chemistry in the former cluster reveals essentially no electrocommunication between the ferrocenyl groups, the latter cluster displays significant redox communication between the two ferrocenyl groups. Treatment of 1,12-bis(ferrocenyl)-1,3,5,7,9,11-dodecahexayne with $Os_3(CO)_{11}$(MeCN) produces the hexaosmium compound $Os_6(CO)_{22}(\mu_6,\eta^8$-Fc$C_4$CCCC$C_4$Fc), whose structure exhibits two open triosmium clusters that are coordinated parallel to opposite sides of

* Tel.: +1 940 565 3548; fax: +1 940 565 3814.
E-mail address: cobalt@unt.edu.

0010-8545/$ – see front matter © 2005 Elsevier B.V. All rights reserved.
doi:10.1016/j.ccr.2005.02.015

the hexayne chain. The reaction of $H_2Os_3(CO)_{10}$ with 1,8-bis(ferrocenyl)octatetrayne yields the following three cluster compounds, $Os_3(CO)_9[\mu_3,\eta^3$-(*E*)-FcCCHC$_4$COCCFc], $Os_3(CO)_{10}(\mu_3,\eta^2$-FcCHCHC$_2$CCCCFc), and $Os_6(CO)_{20}[\mu_6,\eta^4$-(*E*),(*E*)-FcCHCHC$_2C_2$CHCHFc]. The hydrogen transfer step that accompanies these reactions has been crystallographically established, and mechanism for the *trans* hydrogenation at a bimetallic center is discussed [2]. The synthesis of several electron-deficient benzoheterocyclic clusters having the formula $Os_3(CO)_9(\mu_3,\eta^2$-LH)(μ-H) (where L = heterocycle) has been reported. The special μ_3,η^2 bonding mode observed at the C(7) or C(8) position of the carbocyclic ring is discussed. This special bonding mode, along with the protective coordination of the nitrogen center by the cluster, dramatically alters the normally observed heterocycle reactivity towards hydride and hydronium ions. Soft nucleophiles (phosphines) display addition to the metal frame, while the reaction of hard nucleophiles (hydrides and bulky carbanions) takes place by addition to the heterocyclic moiety [3]. New cluster derivatives using $Pd(PBu^t_3)_2$ and $Pt(PBu^t_3)_2$ have been prepared and structurally characterized. Treatment of $Ru_3(CO)_{12}$ with the former reagent affords the tripalladium adduct $Ru_3(CO)_{12}[Pd(PBu^t_3)]_3$. The new FePt mixed-metal carbide clusters $PtFe_4(CO)_{12}$(cod)(μ_5-C) and $PtFe_4(CO)_{12}(PMe_2Ph)_2(\mu_5$-C) have been obtained from the reaction of $[Fe_5(CO)_{14}(\mu_5$-C)]$^{2-}$ with Pt(cod)Cl$_2$ and $Pt(PMe_2Ph)_2Cl_2$, respectively. The synthesis, fluxional behavior, and solid-state structures of $PtRu_5(CO)_{15}(PMe_2Ph)(\mu_6$-C) and $PtRu_5(CO)_{14}(PMe_2Ph)_2$ (μ_6-C) are presented and discussed. The preparation of the bisphosphine cluster $Ru_6(CO)_{14}(PMe_2Ph)_2(\mu_6$-C) is also described. Me$_3$NO-induced decarbonylation of this Ru_6 cluster furnishes the metallated products $Ru_6(CO)_{13}$(μ-PMe$_2$)(μ_3,η^3-Me$_2$PC$_6$H$_4$)(μ_6-C) and $Ru_6(CO)_{14}$(PMe$_2$Ph)(μ,η^2-MePhPCH$_2$)(μ_6-C)(μ-H). Thermolysis of same bisphosphine cluster at 127 °C gives the latter metallated product, along with $Ru_6(CO)_{14}(\mu$-PMe$_2$)(MePhPCH$_2$)-(μ_6-C) and $Ru_6(CO)_{12}(\mu$-PMe$_2)_2(\mu_3,\eta^2$-C$_6$H$_4$)(μ_6-C) [4].

The transmetalation of lanthanide complexes with $Hg[Co(CO)_4]_2$ has been studied. While transmetalation in pyridine, THF, and DME affords discrete ion pairs of the form $[Ln(L)_x][Co(CO)_4]_2$, the use of weak donating solvents such as Et$_2$O gives two-dimensional isocarbonyl arrays of $[(Et_2O)_3Ln\{Co_4(CO)_{11}\}]_\infty$. The heretofore unknown $[Co_4(CO)_{11}]^{2-}$ anion in this complex originates from an oxidation/condensation of $[Co(CO)_4]^-$. Two isomers of $[Co_4(CO)_{11}]^{2-}$ were observed (pseudo-C_{3v} and C_{2v} symmetries). It is shown that $[(Et_2O)_3Yb\{Co_4(CO)_{11}\}]_\infty$ is unstable in the presence of Lewis bases, leading to the disproportionation of the cluster [5]. Treatment of $Mn_2(CO)_7(\mu_2$-S$_2$) with tertiary phosphines and arsines leads to several dimanganese complexes and the polynuclear compounds $Mn_4(CO)_{14}(AsMe_2Ph)_2(\mu_3$-S$_2)_2$, $Mn_6(CO)_{20}(AsMe_2Ph)_2(\mu_4$-S$_2)_3$, and $Mn_4(CO)_{14}$(AsMe$_2$Ph)$_2(\mu_3$-S$_2)_2$. The same Mn_2 complex reacts with $Pt(PPh_3)_2$(PhC$_2$Ph), $CpCo(CO)_2$, CpCo(CO)(PPh$_3$), and $Cp^*Rh(CO)_2$ to furnish the trimetal clusters $Mn_2(CO)_6Pt(PPh_3)_2(\mu_3$-S$)_2$, $CpCoMn_2(CO)_6(\mu_3$-S$)_2$, CpCo$Mn_2(CO)_5(PPh_3)(\mu_3$-S$)_2$, and $Cp^*RhMn_2(CO)_6(\mu_3$-S$)_2$, respectively. X-ray structural analyses confirm the formal insertion of the unsaturated metal species into the S–S bond of the starting dimer. The same Mn_2 starting material has been examined for its reactivity towards thioethers and Me$_2$S, leading to Mn_2 and Mn_4 compounds as the major products [6]. The synthesis and reactivity of bimetallic clusters containing ruthenium are reported. Multiple additions of Ph$_3$SnH to $Ru_6(CO)_{14}(C_6H_6)(\mu_6$-C) produce new RuSn complexes possessing up to five tin ligands. Cluster build-up reactions using $Pt(PBu^t_3)_2$ and $Pd(PBu^t_3)_2$ with $Ru_6(CO)_{17}(\mu_6$-C) and $Ru_5(CO)_{15}(\mu_5$-C) have been explored. The new cluster $PtRu_5(CO)_{15}(PBu^t_3)(\mu_6$-C) has been isolated and fully characterized in solution and by X-ray crystallography. NMR and X-ray studies reveal that this $PtRu_5$ cluster exhibits isomerization behavior involving opened and closed forms that interconvert in solution [7]. The reaction growth-patterns of CO and PR$_3$-ligated bimetallic Au-M clusters (where M = Ni, Pd, Pt) have been investigated. The synthesis and structural characterization of $[Au_7Ni_7(CO)_{10}(PPh_3)_6]^-$ are discussed. The isolation and X-ray structure of the first high-nuclearity thallium-palladium cluster $[Tl_2Pd_{12}(CO)_9(PEt_3)_9]^{2+}$, which was originally thought to be a Au_2Pd_{12} cluster, are reported. The structure-to-synthesis approach affords a near quantitative yield of the Tl_2Pd_{12} cluster from the reaction of Au(SMe$_2$)Cl with $TlPF_6$ and $Pd_4(CO)_{15}(PEt_3)_4$. ^{31}P NMR spectroscopy has been successfully employed in the study of the reversible interconversion between $Pd_{23}(CO)_{20}(PEt_3)_{10}$ and $Pd_{23}(CO)_{20}(PEt_3)_8$. The solution ^{31}P NMR data correlate well with the different metal-core structures adopted by each cluster [8].

2. Homometallic clusters

2.1. Group 6 clusters

Thermolysis of $CpWMo(CO)_7(\mu$-PPh$_2$) with CpW$(CO)_3$(SPh) leads to C–S bond cleavage and formation of the trinuclear complex $CpW(CO)_2(\mu$-S$)_2(\mu$-PPh$_2$)Mo(CO)$_2(\mu$-PPh$_2$)W(CO)$_2$Cp, whose X-ray structure is shown in Fig. 1, along with $CpW(CO)(\mu$-SPh$)_2(\mu$-PPh$_2$)Mo(CO)$_3$. The ability of the SPh moiety to adopt a μ_3-SPh ligation mode is postulated as a means by which the bond dissociation energy of the C–S bond may be decreased, promoting the facile C–S bond cleavage [9].

2.2. Group 7 clusters

Sodium amalgam reduction of $Mn_2(CO)_7(\mu$-S$_2$) produces the new anionic cluster $[Mn_3(CO)_{10}(\mu_3$-S$_2)_2]^-$ in low yield. The same cluster has also been obtained from the

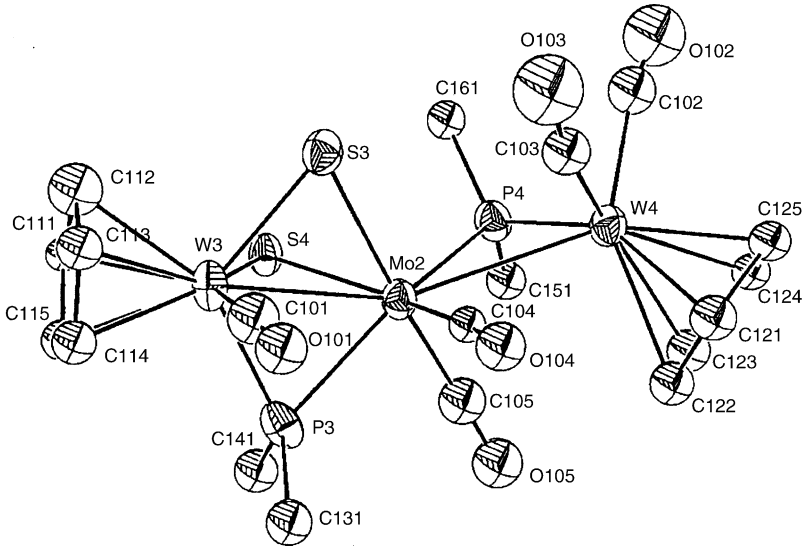

Fig. 1. X-ray structure of $CpW(CO)_2(\mu\text{-}S)_2(\mu\text{-}PPh_2)Mo(CO)_2(\mu\text{-}PPh_2)W(CO)_2Cp$. Reprinted with permission from Organometallics. Copyright 2003 American Chemical Society.

reaction of $Mn_4(CO)_{15}(\mu_3\text{-}S_2)(\mu_4\text{-}S_2)$ with $[Ph_3PMe][I]$ in good yield. Treatment of the anionic Mn_3 cluster with $[CpFe(CO)_2(acetone)]^+$ gives the neutral Mn_3Fe cluster $CpFeMn_3(CO)_{12}(\mu_3\text{-}S_2)(\mu_4\text{-}S_2)$, whose X-ray structure confirms the coordination of the $CpFe(CO)_2$ moiety to a single sulfur atom in one of the two disulfide ligands. The X-ray structure $[Mn_3(CO)_{10}(\mu_3\text{-}S_2)_2]^-$ indicates that the molecular structure is best regarded as an inorganic analogue of quadricyclane [10]. New polynuclear selenido-capped manganese compounds have been synthesized from the phosphine-selenide compounds bis(diphenylphosphino)ethane diselenide, bis(diphenylphosphino)methane monoselenide, and Ph_2MePSe. The reaction between the latter phosphine-selenide reagent and $Mn_2(CO)_8(MeCN)_2$ affords $Mn_4(\mu_3\text{-}Se)_2(\mu\text{-}CO)(CO)_{14}(Ph_2PMe)_2$, whose molecular structure was crystallographically established [11]. The synthesis, characterization, and catalytic reactivity of supported metal clusters have been published. The chemistry of $H_3Re_3(CO)_{12}$, $Os_3(CO)_{12}$, and $Ir_4(CO)_{12}$ at the surface of the support, as well as other cluster compounds, is briefly discussed [12]. Hydrogenation and C–S bond hydrogenolysis of benzothiophene are observed in the reaction with $Re_2(CO)_{10}$ and $H_4Re_4(CO)_{12}$. Treatment of the heterocycle with $Re_2(CO)_{10}$ under H_2 gives the trirhenium cluster $Re_3(CO)_9(\mu\text{-}H)_2(\mu_3\text{-}S\text{-}2\text{-}EtC_6H_4)$($\mu$-2,3-dihydrobenzothiophene). The presence of the hydrogenated benzothiophene ligand and a thiolate moiety derived from the hydrogenation and cleavage of a C–S bond in the benzothiophene substrate has been confirmed by X-ray analysis (Fig. 2). Mechanistic data show that the reaction actually proceeds from $H_3Re_3(CO)_{12}$, followed by transformation to $H_4Re_4(CO)_{12}$ and then reaction with the heterocyclic substrate [13].

2.3. Group 8 clusters

Broad-band UV irradiation of $Ru_3(CO)_{12}$ in the presence of acryloyl polystyrene resins gives the corresponding polymer-bound $Ru(CO)_4$ species via attachment to the pendant alkene linkage. The stability of the polymer-supported complex was examined as an organometallic synthon [14]. The results of a study on the ν(CO) vibrational spectra of several planar metal clusters containing $M(CO)_4$ groups have been published. Good qualitative agreement of the band

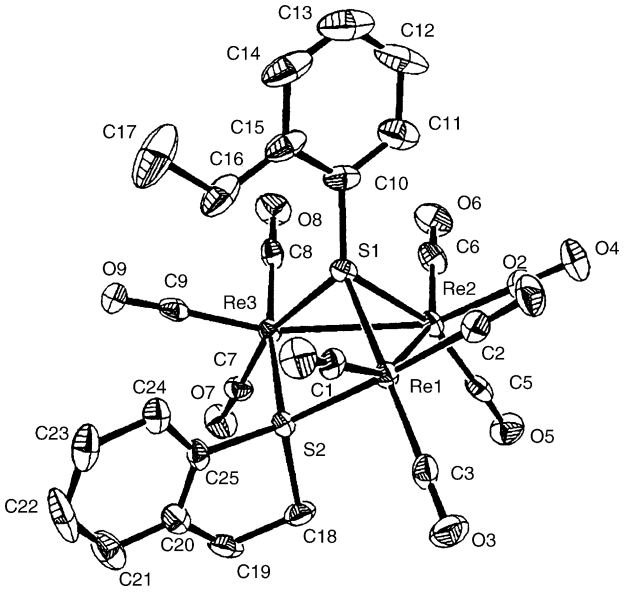

Fig. 2. X-ray structure of $Re_3(CO)_9(\mu\text{-}H)_2(\mu_3\text{-}S\text{-}2\text{-}EtC_6H_4)$($\mu$-2,3-dihydrobenzothiophene). Reprinted with permission from Inorganic Chemistry. Copyright 2003 American Chemical Society.

intensity changes as a function of the number of metals and the adopted cluster geometry is found in both the infrared and Raman spectra. Spectral assignments are discussed with respect to the spherical harmonic model (SHM) and the tensor harmonic model (THM). The agreement exhibited by these two cluster bonding models is related to the size of the metal cluster, with the former model successfully accounting for the spectroscopic properties of larger metal clusters [15]. The cluster compounds $M_3(CO)_{12}$ (where M = Fe, Ru, Os) have been reanalyzed in terms of a model based on σ-aromaticity using Hückel and Mobius topological treatments. The cluster $Pt_3(CO)_3(\mu\text{-}CO)_3$ has also been analyzed by using the same methods, with no 3c–4e Mobius surface bonding observed due to the bridging CO groups. The relationship of σ-aromaticity to three-dimensional aromaticity found in deltahedral boranes and related octahedral metal clusters is discussed [16]. A reproducible high-yield synthesis of $Ru_3(CO)_{12}$, $H_4Ru_4(CO)_{12}$, and $[Ru_6(\mu_6\text{-}C)(CO)_{16}]^{2-}$ from $RuCl_3{\cdot}nH_2O$ has been published. The end-product obtained is controlled by the alkali carbonate additive, the gas-phase composition (CO or CO/H_2), and the reaction temperature [17].

The oxidative cyclization of 4-penten-1-ols to dihydrofurans in the presence of CO has been demonstrated when $Ru_3(CO)_{12}$ was employed as a catalyst precursor [18]. The tandem isomerization/Claisen rearrangement of dienyl ethers to γ,δ-unsaturated aldehydes has been achieved by using the component catalyst systems $Ru_3(CO)_{12}$/diimine/$CsCO_3$ [19]. Treatment of $Ru_3(CO)_{12}$ with chiral diiminodiphosphine tetradentate ligands yields chiral monoruthenium complexes that function as catalysts for the asymmetric transfer hydrogenation of ketones. The hydrogenation of propiophenonate to 1-phenyl-1-propanol occurs with a 96% e.e. The analogous reactions employing $Ru_3(CO)_{12}$ with BINAP and DIOP were unsuccessful, as was the cluster $H_4Ru_4(CO)_{12}$ in the presence of the chiral ligand *N*,*N*′-bis[*o*-(diphenylphosphino)benzylidene]-1,2-diphenylethylenediamine [20]. The reaction of $Ru_3(CO)_{12}$, phosphine, and various dioxolene ligands affords the mononuclear complexes $RuP_2(CO)_2L$ and $[\{RuP_2(CO)_2\}_2(L)]^+$ (where L = dioxolene). The spectroscopic data and mixed-valence properties of these new compounds are discussed [21]. Fragmentation of $Ru_3(CO)_{12}$ and $H_4Ru_4(CO)_{12}$ is observed upon treatment with bis(2-pyridyl)amine and its conjugate base. Here the major product is the diruthenium complex $Ru_2(dpa)_2(CO)_4$ [22]. Dibenzothiophene has been allowed to react with $Ru_3(CO)_{12}$ in refluxing heptane to produce $Ru_2(C_{12}H_8)(\mu\text{-}CO)(CO)_5$. X-ray analysis of the product confirms the double C–S bond activation/desulfurizaton process attendant in this reaction. The reactivity of 3-methyl and 2-methyldibenzothiophene with $Ru_3(CO)_{12}$ exhibits a similar reactivity pattern as the parent heterocycle [23]. Treatment of $Fe_3(CO)_{12}$ with α,β-unsaturated ketones containing β-substituted thiol groups leads to cluster fragmentation and formation of $Fe_2(CO)_6[\mu\text{-}S_2C{=}CHC(O)C_6H_4X]$. The X-ray structure of the fluoro derivative accompanies this report [24]. Fluorination of $Os_3(CO)_{12}$ in HF/SbF_5 gives the mononuclear complex $Os(CO)_4(FSbF_5)_2$, whose X-ray structure reveals that both SbF_6 moieties occupy *cis* positions in the octahedron. The reactivity of $Ir_4(CO)_{12}$ towards fluorination under similar conditions has also been examined, with [*fac*-$Ir(CO)_3(FSbF_5)_2HF]SbF_6{\cdot}HF$ and *mer*-$Ir(CO)_3F(FSbF_5)_2$ being isolated and structurally characterized [25].

9-Anthraldehyde oxime reacts with $Os_3(CO)_{11}(MeCN)$ to give $Os_3(CO)_{11}$(9-anthracenecarbonitrile) in moderate yields as a result of the formal dehydration of the oxime moiety. The same product is furnished in high yields from the reaction of $Os_3(CO)_{11}(MeCN)$ with 9-anthracenecarbonitrile. Carbonylation and hydrogenation reactions with this new nitrile-substituted cluster produce $Os_3(CO)_{12}$ and $H_2Os_3(CO)_{10}$, respectively. The UV–vis data for $Os_3(CO)_{11}$(9-anthracenecarbonitrile) exhibit intense MLCT absorptions that are discussed relative to the electronic transitions from the Os–Os sigma bonding molecular orbitals to the anthracene π^* system [26]. The reactivity of acenaphthylene with $Os_3(CO)_{10}(MeCN)_2$ at room temperature has been studied. The sole observed product was found to be $Os_3(CO)_{10}(\mu\text{-}H)(\mu,\eta^2\text{-}C_{12}H_7)$, whose X-ray structure reveals a σ–π coordinated acenaphthyl ligand that bridges one edge of the Os_3 frame. Thermolysis of this initial product affords $Os_3(CO)_9(\mu\text{-}H)_2(\mu_3,\eta^2\text{-}C_{12}H_6)$. Continued heating of this latter Os_3 cluster in the presence of added acenaphthylene at 160 °C yields the new osmium compounds $Os_4(CO)_{12}(\mu_4,\eta^2{:}\eta^2\text{-}C_{12}H_6)$, $Os_2(CO)_6(\mu,\eta^4\text{-}C_{24}H_{12})$, $Os_3(CO)_9(\mu\text{-}H)(\mu_3,\eta^2\text{-}C_{24}H_{13})$, and $Os_2(CO)_5(\mu,\eta^4\text{-}C_{24}H_{12})(\eta^2\text{-}C_{12}H_8)$. The solid-state structures of these last four products have been solved by X-ray crystallography [27]. The catalytic isomerization of hexamethyl Dewar benzene to hexamethylbenzene by $Os_3(CO)_{10}(MeCN)_2$ has been investigated. The isomerization reaction is shown to be in competition with ring opening of the substrate to $Os_3(\mu\text{-}H)_2(CO)_9[\mu,\eta^3\text{-}CH(C_6Me_6)]$ and $Os_3(\mu\text{-}H)(CO)_9[\mu_3,\eta^2\text{-}C_2(C_4H_4Et)]$. The unequivocal identity of these latter two Os_3 clusters has been determined (Fig. 3), with a plausible reaction sequence discussed in terms of a cyclobutenylacetylide intermediate [28].

The arene-substituted clusters $[H_3Ru_3(C_6H_6)(C_6H_2Me_4)_2(O)]^+$ and $[H_3Ru_3\{C_6H_5(CH_2)_2OH\}(C_6H_2Me_4)_2(O)]^+$ have been prepared from the precursor compound $[H_3Ru_2(C_6H_2Me_4)]^+$ and its reaction with the dications $[Ru(C_6H_6)(H_2O)_3]^{2+}$ and $[Ru\{C_6H_5(CH_2)_2OH\}(H_2O)_3]^{2+}$. The relationship between the two products and the known cluster $[H_3Ru_3(C_6H_6)(C_6Me_6)_2(O)]^+$ is discussed [29]. The synthesis and structure of the chiral cluster (*S*)-$[H_3Ru_3\{C_6H_5(CHMeCH_2OH)\}(C_6Me_6)_2(O)]^+$ have been published [30]. The use of the triruthenium complex $Ru_3(\mu_3\text{-}O)(\mu\text{-}OAc)_6(bpy)_2(CO)$ as a molecular building block in the construction of molecular multilayers on a Au surface is described. The functionalized Au surface has been characterized by cyclic voltammetry, chronocoulometry, and FT-IR spectroscopy [31]. Treatment of the dinuclear complex $[H_3Ru_2(C_6Me_6)_2]^{2+}$ with

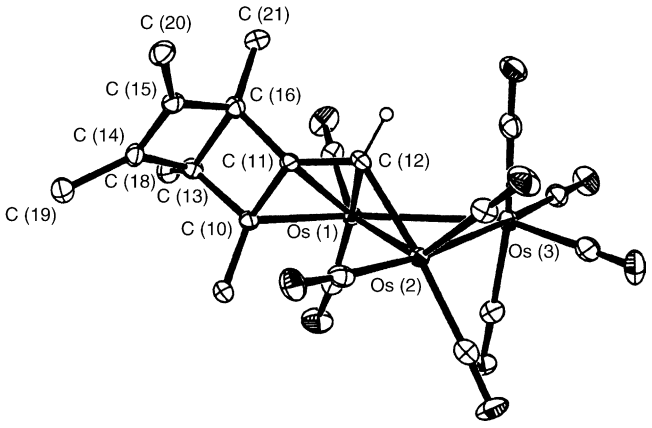

Fig. 3. X-ray structure of $Os_3(\mu\text{-}H)_2(CO)_9[\mu,\eta^3\text{-}CH(C_6Me_6)]$. Reprinted with permission from Organometallics. Copyright 2003 American Chemical Society.

$[Ru(Fc\text{-}arene)(H_2O)_3]^{2+}$ furnishes the ferrocenyl-containing oxo-capped cluster $[H_3Ru_3(Fc\text{-}arene)(C_6Me_6)_2(O)]^+$, whose water solubility has been exploited in the hydrogenation of benzene to cyclohexane under biphasic conditions [32]. Methylidyne–diyne coupling reactions at a triruthenium cluster have been demonstrated. Symmetric diynes react with $Ru_3(\mu\text{-}H)(\mu\text{-}COMe)(CO)_{10}$ to give the regioisomers $Ru_3(\mu\text{-}H)(\mu_3,\eta^3\text{-}MeOCCR{=}CCCR)(CO)_9$ and $Ru_3(\mu\text{-}H)[\mu_3,\eta^3\text{-}MeOCC(CCR){=}CR](CO)_9$ (where R = Me, Ph, CH_2OPh) as a result of insertion of one of the alkyne moieties of the diyne into the Ru–C bond of the methylidyne ligand. The solid-state structures of the two regioisomers formed from the reaction using 2,4-hexadiyne are presented [33]. The cluster compound $(\mu\text{-}H)Ru_3(CO)_9(\mu_3,\eta^3\text{-}C_3H_3)$ has been isolated from the reaction of $Ru_3(CO)_{12}$ with the alkynes diethylaminopropyne and trimethylsilylpropargyl alcohol. X-ray crystallographic analysis confirms the presence of an allylic moiety that is σ-bonded to two ruthenium centers and π-bound to the third ruthenium atom [34]. Two isomers of $Os_3(\mu\text{-}H)(CO)_{10}[\mu_3,\eta^1{:}\eta^3{:}\eta^1\text{-}Ph(C)C_6H_6]$, which were obtained from the reaction of $H_2Os_3(CO)_{10}$ and 1,4-diphenylbuta-1,3-diyne, have been spectroscopically and crystallographically characterized. Both isomers exhibit an open metal triangle and an unusual pseudo-allylic interaction involving a fused six- and five-membered ring system resulting from the ring-closure reaction of the diyne. Thermolysis leads to CO loss and formation of a closed Os_3 triangular frame. A plausible reaction sequence accounting for the formation of the observed products is presented and discussed [35]. The reactivity of several different pyrones with $Os_3(CO)_{10}(MeCN)_2$ has been investigated. The different coordinative bonding modes adopted by the pyrone ligands were established by solution NMR measurements and X-ray crystallography [36]. The reaction of $H_2Os_3(CO)_{10}$ with conjugated diynes containing a nucleophilic oxygen atom [$PhC_2C_2CH_2OH$ and $PhC_2C_2C(O)Ph$] has been examined. Diyne coordination to the triosmium cluster, followed by intramolecular cyclization with the nucleophilic β-oxygen atom, leads to furan rings that are coordinated to the cluster. These products exhibit the generalized structures $HOs_3(CO)_{10}[\mu,\eta^1{:}\eta^2\text{-}PhCH_2(C{=}CH{-}C{=}CH{-}O)]$ and $HOs_3(CO)_{10}[\mu,\eta^1{:}\eta^1\text{-}Ph(C{=}CH{-}C{=}C{-}O)CPh]$. Thermolysis of the latter cluster results in CO dissociation and formation of $HOs_3(CO)_9[\mu_3,\eta^1{:}\eta^3{:}\eta^1\text{-}Ph(C{=}CH{-}C{=}CH{-}O)CPh]$, whose X-ray structure (Fig. 4) reveals a closed C_3Os_3 five-vertex pyramidal core. $H_2Os_3(CO)_{10}$ reacts with $Me_2(HO)CC_2C_2CMe_2(OH)$ without cyclization to furnish $Os_3(CO)_{10}(\mu_3,\eta^2\text{-}RCH{=}CH{-}CHC_2R)$ and $Os_3(CO)_{10}(\mu_3,\eta^2\text{-}RC_2C_2R)$. The results of deuterium-labeling studies are used in the formulation of a working reaction scheme [37].

The reactivity of $Cp^*{}_3Ru_3(\mu\text{-}H)_3(\mu_3\text{-}H)_2$ with a variety of reducing agents has been investigated. The reaction with Et_2Zn affords the new cluster $Cp^*{}_3Ru_3(\mu\text{-}H)_3(\mu_3\text{-}ZnEt)(\mu_3\text{-}H)$, while Et_3Al reacts with the starting cluster to give $Cp^*{}_3Ru_3(\mu\text{-}H)_3(\mu_3\text{-}AlEt)$. The X-ray structures of three products accompany this report [38]. Thermolysis of the triruthenium clusters $(Cp^*Ru)_2Cp^*Ru(CRCR'CHCH)$ promotes isomerization to $(Cp^*Ru)_2Cp^*Ru(CHCRCR'CH)(\mu\text{-}H)_3$. These reactions were studied by NMR spectroscopy, which allowed for the evaluation of the activation parameters associated with these reactions. The molecular structure of $(Cp^*Ru)_2Cp^*RuCH[C(Me)CHCH](\mu\text{-}H)_3$ has been determined, confirming the presence of the ancillary 3-methylruthenacyclopentadiene moiety in the product as a result of CMe group isomerization. Computational studies have been carried out in order to probe the likely path associated with pentadiene ligand isomerization. A process involving a cyclobutadiene intermediate is ruled out, on the basis of the MO data. A mechanism involving (1) C=C double bond insertion into a Ru–H bond, (2) C–C bond cleavage to produce an allyl–methylene complex, (3) reductive coupling to generate the ruthenacylopentadiene ring, and (4) C–H bond cleavage to give the final product is supported by MO calculations and is in agreement with the experimentally measured $\Delta H^{\neq}$ values found by NMR spectroscopy [39]. A report describing the oxidatively induced bimetallic reductive C–C bond coupling of a μ_3-allyl ligand has appeared. Treatment of $(Cp^*Ru)_3(\mu\text{-}H)_4[\mu_3,\eta^3\text{-}C(H)C(H)CMe]$ with two equivalents of $[Cp_2Fe][PF_6]$ produces the η^3-cyclopropenyl-substituted cluster $[(Cp^*Ru)_3(\mu\text{-}H)_3\{\mu_3,\eta^3\text{-}C_3H_2Me\}]^+$ in quantitative yield. Cyclic voltammetric data support a sequence involving an oxidation of the starting cluster to the corresponding $47e^-$ species, followed by a rearrangement and deprotonation. The structural identity of the cationic product was ascertained by ^1H NMR measurements and X-ray diffraction analysis. The results of a density functional study on the model cluster $[(Cp^*Ru)_3(\mu\text{-}H)_3(\mu_3,\eta^3\text{-}C_3H_3)]^+$ are presented, with the nature of the cluster-cyclopropenyl ring bonding fully dissected [40].

The room temperature reaction of $Os_3(CO)_{10}(MeCN)_2$ with 2,4,5-trimethylthiazole in CH_2Cl_2 produces the new isomeric compounds $HOs_3(CO)_{10}[\mu,\eta^2\text{-}CH_2C{=}NC(Me){=}C(Me)S]$ and $HOs_3(CO)_{10}[\mu,\eta^2\text{-}CH_2C{=}C(Me)SC(Me)$

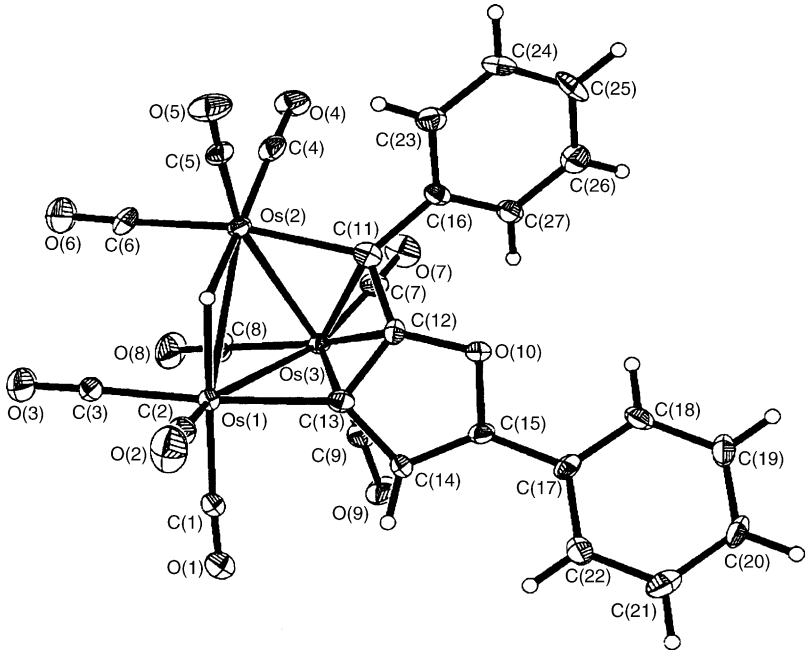

Fig. 4. X-ray structure of $HOs_3(CO)_9[\mu_3,\eta^1{:}\eta^3{:}\eta^1$-Ph(C=CH–C=CH–O)CPh]. Reprinted with permission from Organometallics. Copyright 2003 American Chemical Society.

=N], along with the known clusters $HOs_3(CO)_{10}(\mu$-Cl) and $HOs_3(CO)_{10}(\mu$-OH). The two new clusters, which are formed by activation of the C-2 and C-4 substituents, respectively, undergo decarbonylation and a second C–H bond activation of the coordinated methylidene moiety to give $H_2Os_3(CO)_9[\mu_3,\eta^2$-CHC=NC(Me)=C(Me)S] and $H_2Os_3(CO)_9[\mu_3,\eta^2$-CHC=(Me)SC(Me)=N] upon heating. All new products were fully characterized in solution by IR and NMR spectroscopies and mass spectrometry. The X-ray structures of two clusters are presented and discussed with respect to their spectroscopic properties [41]. Nitrogen-nitrogen bond cleavage has been achieved in the reaction between $(Cp^*Ru)_3(\mu$-H$)_3(\mu_3$-H$)_2$ and monosubstituted hydrazines. Here the nonsymmetrically capped bis(μ_3-imido) clusters $(Cp^*Ru)_3(\mu$-NR$)(\mu_3$-NH$)(\mu$-H) are obtained as the major products. The same starting cluster was also investigated for its reactivity towards 1,2-diphenylhydrazine, giving the monocapped imido cluster $(Cp^*Ru)_3(\mu$-H$)_3(\mu_3$-NPh) as the sole observed product. Kinetic studies employing methylhydrazine confirm that the cluster initially coordinates the ligand at the more nucleophilic MeNH terminus rather than the more sterically accessible NH_2 site. The kinetic data and spectroscopic studies have allowed for the construction of a working mechanism involving the cooperative action of all three ruthenium centers. The molecular structures of three X-ray compounds have been solved and their structural highlights discussed [42]. Treatment of $Ru_3(CO)_{12}$ with bis(2-pyridyl)ketone oxime in refluxing THF produces $Ru_3(CO)_8(\mu,\eta^3$-dpko-N,N,O) and $Ru_3(CO)_4(\mu,\eta^3$-dpko-N,N,O$)_2$. Both complexes are doubly bridged by the two dpko ligands, which are attached to one Ru center via the oximate oxygen atom and chelated to the other two Ru centers through the pyridyl and oximate nitrogen groups. Reaction of same ligand with $M_3(CO)_{10}(MeCN)_2$ (where M = Ru, Os) at room temperature gives $M_3(\mu$-H$)(\mu,\eta^3$-dpko-N,N,O$)(CO)_9$. The reactivity of these oximate complexes as DNA cleavage reagents was found to be poor. The solid-state structures of four compounds have been determined [43]. The influence of the bridging carbonyl groups on the bonding, photochemical, and electrochemical properties of $Ru_3(CO)_8(\mu$-CO$)_2(\alpha$-diimine) (where diimine = 2,2′-bpy, 4,4′-Me$_2$-bpy, 2,2′-bpm) has been investigated. Optical excitation at 471 nm leads to the population of a $\sigma(Ru_3)\pi^*(\alpha$-diimine) excited state that undergoes a rapid decay to a π(Ru/μ-CO)$\pi^*(\alpha$-diimine) lowest excited state. These spectroscopic assignments are supported by resonance Raman and picosecond time-resolved infrared spectra and theoretical MO calculations at the DFT level. The effect of the reaction solvent in promoting cluster-opening and electron-transfer reactions is outlined [44]. The reaction of the azavinylidene-bridged cluster $HRu_3(CO)_{10}(\mu$-N=CPh$_2$) with the diphosphine ligands dpme and bpcd has been explored. Both ligands replace two CO groups to give $HRu_3(CO)_8(\mu$-N=CPh$_2$)(P–P). The former ligand bridges the two ruthenium centers that are also bridged by the ancillary hydride ligand, while the latter ligand chelates to one of the hydride-bridged ruthenium centers at an axial and equatorial site. The molecular structures of both products were established by X-ray crystallography [45]. The synthesis, spectroscopic characterization, and DNA binding affinities of several water-soluble benzoheterocycle triosmium clusters have been published. The benzoheterocyclic ligands used in the coordination of the Os_3 core were 3-aminoquinoline, 3-(2-phenylacetimido)quinoline, and phenanthridine, with

the ancillary phosphorus ligands $Na_3[P(C_6H_4SO_3)_3]$ and $[P(OCH_2CH_2NMe_3)_3][I_3]$ being used to control the degree of aggregation in aqueous solution and overall aqueous stability. The data from plasmid super coiled DNA relaxation tests employing a 1% electrophoresis agarose gel are presented and discussed. The preliminary results from these DNA binding affinity studies do indeed support a relationship between the nature of the attached heterocycle and DNA binding affinity [46]. The reactivity of $Os_3(CO)_{10}(MeCN)_2$ with a series of aminothiazole compounds has been explored. Included in this report are the X-ray diffraction structures of the new cluster compounds $Os_3(\mu\text{-}H)(CO)_{10}(\mu\text{-}C_8H_7N_2S)$, $Os_3(\mu\text{-}H)(CO)_9(\mu_3,\eta^2\text{-}C_3H_5N_2S)$, and $Os_3(\mu\text{-}H)(CO)_9(\mu_3,\eta^2\text{-}C_6H_7ON_2S)$ [47]. The thermolysis reaction between $Ru_3(CO)_{12}$ and 2-mercaptobenzothiazole has been reexamined, yielding the known cluster $HRu_3(CO)_9(\mu_3,\eta^2\text{-}C_7H_4NS_2)$ and the new compound $H_2Ru_3(CO)_7(\mu_3,\eta^2\text{-}C_7H_4NS_2)(\mu,\eta^2\text{-}C_7H_4NS_2)$. This latter cluster has been isolated and fully characterized in solution and by X-ray crystallography. One of the main structural highlights found for this cluster includes a triangular array of ruthenium atoms that exhibits three statistically different Ru–Ru bond distances. Treatment of former known cluster with excess 2-mercaptobenzothiazole at 68 °C affords the same H_2Ru_3 cluster [48]. A facile and efficient one-pot synthesis of a hexaruthenium cluster from $Ru_3(CO)_{12}$ and 2-aminopyridine has been reported. The initial product from these reactions is the pyridine-coordinated triruthenium cluster $HRu_3(CO)_9(\mu_3\text{-ampy})$, which undergoes further reaction with $Ru_3(CO)_{12}$ to furnish $Ru_6(\mu_3\text{-}H)_2(CO)_{14}(\mu\text{-}CO)_2(\mu_5,\eta^2\text{-ampy})$ in good yield. The role of the ancillary 2-aminopyridine-derived ligand in helping maintain the Ru_6 core and facilitating CO substitution processes is discussed [49]. The formation of a highly functionalized azulene ligand has been observed in the reaction of $HRu_3(CO)_9(\mu_3,\eta^2\text{-ampy})$ with diphenylbutadiyne (2 eq.) and 2,4-hexadiyne (1 eq.). Here the product $Ru_2(\mu,\eta^8\text{-}C_{38}H_{26})(CO)_5$ has been characterized in solution and by X-ray diffraction analysis. The ancillary 1-(phenylethynyl)-2,4-diphenyl-5-(propyn-1-yl)-6-methyl-7,8-benzoazulene ligand is bound to the $Ru_2(CO)_5$ moiety in a manner identical to that found in $Ru_2(\mu,\eta^8\text{-azulene})(CO)_5$ [50]. $Os_3(CO)_{10}(MeCN)_2$ has been allowed to react with 2,2′-diamino-1,1′-binaphthalene to give the coordinatively unsaturated cluster $HOs_3(CO)_9(\mu_3,\eta^2\text{-Hbinam-N,C})$, whose X-ray structure confirms the presence of a C-metalated Hbinam ligand that is bound to one osmium center via an NH_2 group and to the other two osmium atoms through the metalated C atom. The reaction of $Ru_3(CO)_{10}(MeCN)_2$ with H_2binam at room temperature did not lead to any observable product. The reaction of LiHbinam with $Ru_3(CO)_{12}$, followed by treatment with $[HOEt_2][BF_4]$, furnishes $HRu_3(CO)_{10}(\mu,\eta^1\text{-Hbinam})$. Spectroscopic data indicate that the Hbinam ligand functions as an edge-bridging amido ligand. The same cluster reacts with added dppm to give $H_2Ru_3(CO)_7(\mu_3,\eta^2\text{-binam})(\mu,\eta^2\text{-dppm})$. The X-ray

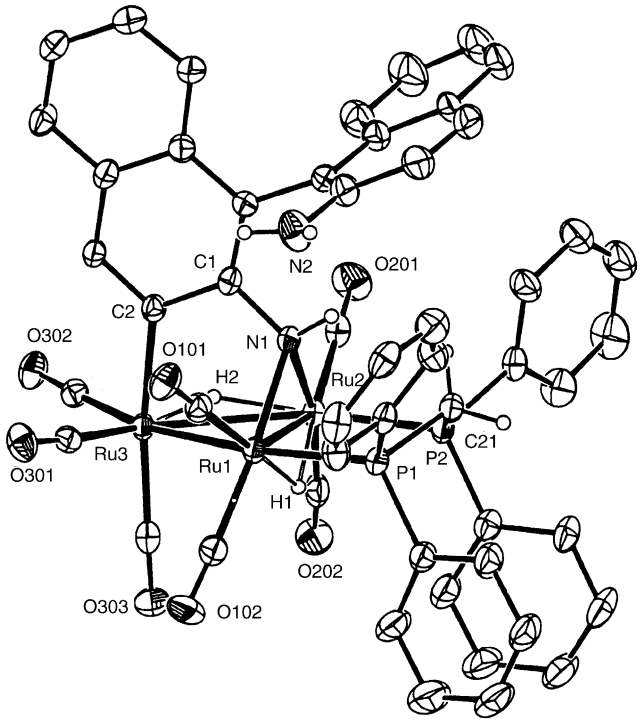

Fig. 5. X-ray structure of $H_2Ru_3(CO)_7(\mu_3,\eta^2\text{-binam})(\mu,\eta^2\text{-dppm})$. Reprinted with permission from Organometallics. Copyright 2003 American Chemical Society.

structure (Fig. 5) reveals that dppm coordination induces a C–H bond activation of the amido-bound naphthalene ring. A proposed mechanism showing site-selective coordination of the dppm ligand at the hydride-bridged Ru–Ru bond, followed by C–H bond oxidative addition, is presented and discussed [51].

The reaction of 2,4,6-tris(trimethoxy)phenylphosphine sulfide and 1,2-bis[(diphenylphosphino)methyl]benzene sulfide with $Ru_3(CO)_{12}$ yields new phosphine-substituted sulfido-capped clusters possessing Ru_3S, Ru_3S_2, and Ru_4S_2 polyhedral cores. The four X-ray structures that accompany this report are discussed relative to known sulfido-capped ruthenium clusters [52]. The new carbene cluster $Ru_3(\mu_3\text{-Se})(\mu_3\text{-}H)(\mu_2\text{-}PPh_2)(CO)_6(\mu_2\text{-}CHC_6H_4CH_2PPh_2)$ has been synthesized from $Ru_3(CO)_{12}$ and 1,2-bis[(diphenylphosphino)methyl]benzene diselenide. Treatment of $Ru_3(CO)_{12}$ with 1,2-bis[(diphenylphosphino)methyl]benzene leads only to carbonyl substitution by the diphosphine ligand without ligand fragmentation, confirming the importance of selenium in promoting the formation of the carbene moiety. The fluxional properties of the ancillary ligands in several product clusters have been explored by COSY, NOESY, and TOCSY 2D NMR measurements. The solution NMR data are discussed with respect to the solid-state structure of the products [53]. A report dealing with the quantitative analysis of ligand effects (QALE) related to the associative reactions of phosphines with $Ru_3(CO)_{12}$ has been published. Besides the normal contributions of ligand electronic and steric effects on the rate of the reaction, the addition of phosphite π-acidity

and an aryl group effect allows for an accurate quantitation of the rate data by regression analysis. The construction of a $\log k_2$ surface provides a clear visualization of the effects related to σ donation, steric parameters, π-acidity, and aryl group participation of each ligand on the transition state of the substitution reaction [54]. Thermolysis of $Ru_3(CO)_{12}$ with the diphosphine ligand 2,3-bis(diphenylphosphino)-*N*-phenylmaleimide in toluene at 100 °C leads to cluster fragmentation and formation of the donor–acceptor complex $Ru_2(CO)_6$(bppm) and the phosphido-bridged complex $Ru_2(CO)_6[\mu\text{-}C{=}C(PPh_2)C(O)N(Ph)C(O)](\mu_2\text{-}PPh_2)$. Both compounds have been isolated and fully characterized in solution and by X-ray diffraction analysis in the case of the former compound. The reactivity of the bppm ligand is contrasted with the related diphosphine ligands bma and bpcd [55]. Several new diruthenium complexes have been prepared by heating $Ru_3(CO)_{10}(\mu\text{-dppm})$ with the dithiols 1,2-ethanedithiol, 1,3-propanedithiol, and 3,4-toluenedithiol. The compounds isolated from these reactions were $Ru_2(CO)_4(\mu\text{-}SCH_2CH_2S)(\mu\text{-dppm})$, $Ru_2(CO)_4(\mu\text{-}SCH_2CH_2CH_2S)(\mu\text{-dppm})$, and $Ru_2(CO)_4(\mu\text{-}SC_6H_3(Me)S)(\mu\text{-dppm})$, respectively. Protonation of the Ru–Ru bond using HBF_4 affords the corresponding cationic hydride complex. Two X-ray structures accompany this report [56]. The oxidative addition reactivity of diphosphazane monosulfides $Ph_2PN(R)P(S)Ph_2$ [where R = (S)-CHMePh, Pr^i] with $Ru_3(CO)_{12}$ has been investigated. The major products isolated from these reactions are the sulfido-capped clusters $Ru_3(\mu\text{-}CO)(CO)_7(\mu_3\text{-}S)[Ph_2PN(R)PPh_2\text{-}\kappa^2P,P]$, which contain a chelating diphosphazane ligand. This rare coordination mode found for the diphosphazane ligand was confirmed by spectroscopic data and X-ray crystallographic analysis of the chiral diphosphazane derivative [57]. The electrochemical properties of $Ru_3(CO)_8(\mu\text{-dppf})_2$, $Ru_3(CO)_{10}(\mu\text{-dppf})$, and $[Ru_3(CO)_{11}(\mu\text{-dppf})Ru_3(CO)_{11}]$ have been studied by cyclic voltammetry. The X-ray structure of the open-bridged cluster $[Ru_3(CO)_{11}]_2(\mu\text{-dppf})$ is included in this report [58]. The acetylide cluster $HRu_3(CO)_9(\mu_3,\eta^2,\eta^2,\eta^1\text{-}C_2Ph)$ undergoes CO substitution with bpcd in the presence of Me_3NO to give the chelated cluster $HRu_3(CO)_7(bpcd)(\mu_3,\eta^2,\eta^2,\eta^1\text{-}C_2Ph)$ and the zwitterionic cluster $HRu_3(CO)_7[\mu_3,\eta^2,\eta^2,\eta^1,\eta^1,\eta^1\text{-}Ph_2PC{=}CC(O)CH_2C(O)PPh_2C{=}CPh]$. The bpcd ligand is bound to the ruthenium center that is σ-bound by the acetylide ligand in the former product. In the zwitterionic product one of the PPh_2 groups is attached to the acetylide C_α carbon and the other PPh_2 moiety is bound to one of the hydride-bridged ruthenium centers, as shown verified by X-ray diffraction analysis (Fig. 6). Whereas the zwitterionic cluster decomposes during thermolysis, heating the former product leads to oxidative cleavage of one of the P–Ph bonds of the bpcd ligand, followed by reductive coupling with the acetylide ligand. The unequivocal identity of the resulting product, $Ru_3(CO)_7(\mu,\eta^2,\eta^1\text{-}PhC{=}ChPh)[\mu_2,\eta^2,\eta^1\text{-}PhPC{=}CC(O)CH_2C(O)PPh_2]$, was ascertained by solution IR and NMR spectroscopies and X-ray crystallography. A labeling study employing $HRu_3(CO)_7(bpcd)(\mu_3,\eta^2,\eta^2,\eta^1\text{-}C_2tol\text{-}p)$ supports a reaction pathway that involves hydride transfer to a coordinated $PhC_2tol\text{-}p$ ligand [59].

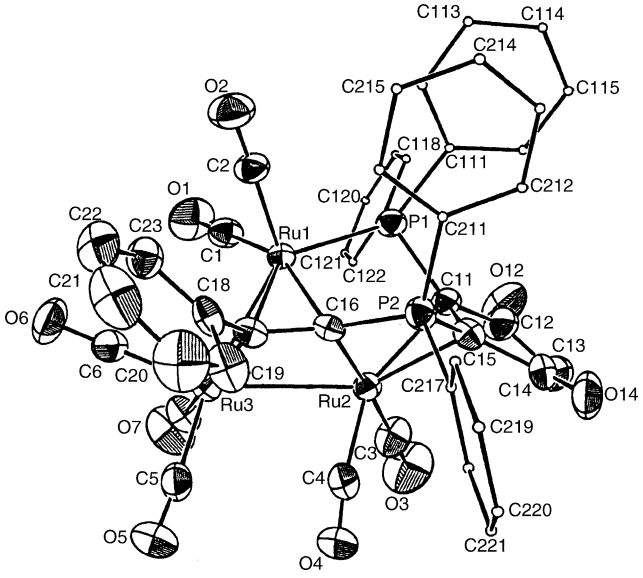

Fig. 6. X-ray structure of $HRu_3(CO)_7[\mu_3,\eta^2,\eta^2,\eta^1,\eta^1,\eta^1\text{-}Ph_2PC{=}CC(O)CH_2C(O)PPh_2C{=}CPh]$. Reprinted with permission from Organometallics. Copyright 2003 American Chemical Society.

The functionalized clusters $Fe_3(\mu_3\text{-}SbR)(\mu_3\text{-}E)(CO)_9$ (where R = Cp^*, $\eta^5\text{-}C_5H_4Bu^t$; E = Se, Te) have been synthesized from $[Fe_3(\mu_3\text{-}E)(CO)_9]^{2-}$ and $RSbX_2$. The related bismuth-capped cluster $Fe_3[\mu_3\text{-}BiFe(CO)_2(\eta^5\text{-}C_5H_4Bu^t)](\mu_3\text{-}Se)(CO)_9$ was prepared by using similar methodology. The spectral and diffraction data associated with these iron clusters are discussed [60]. A microreview dealing the structures, fluxional properties, and reactivity of several phosphine-substituted selenido-capped iron and ruthenium clusters has been published [61]. The kinetics and mechanistic study on the carbonylation of methanol to produce methyl formate have been investigated by using the anionic clusters $[Fe_3(CO)_9E]^{2-}$ (where E = S, Se, Te) as catalysts. The kinetic data support a sequence that is first order in cluster concentration and quasi-second order in CO pressure. This latter dependence suggests a mechanism involving a polyhedral expansion of the initial cluster through metal–metal bond cleavage. Plausible reaction pathways are presented and fully discussed [62].

Treatment of $Fe_2(CO)_9$ with *N*-(2-thienylmethylidene)-2-thienylamine produces the dinuclear cyclometallated complex $Fe_2(CO)_6(R\text{-}C_4HS\text{-}CH_2NCH_2\text{-}C_4H_3S)$ and the two linear tetrairon isomers $Fe_4(CO)_8(\mu\text{-}CO)_2(R\text{-}C_4HS\text{-}CH{=}NCH_2\text{-}C_4H_3S)$, which possess μ,η^1-thienyl β-C:π^1-N and η^2-thienyl, β-C=C:η^2-C=N coordinated organic ligands. The two $66e^-$ clusters adhere to closed valence molecular orbital rules and are isolobally related to $[CpFe(CO)(\mu\text{-}CO)]_2$. Heating the two Fe_4 clusters leads to decomposition, with no isomerization observed. The X-ray structures of these Fe_4 clusters are included in this report [63].

The tetrasubstituted clusters $H_4Ru_4(CO)_8(PMe_2Ph)_4$ and $H_2Ru_4(CO)_9(PMe_2Ph)_4$ have been synthesized and examined by ^1H and ^{31}P NMR spectroscopy. The former cluster displays two isomers in solution that are attributed to clusters with D_{2d} and C_s symmetries. The NMR properties of these isomers are discussed with respect to how the hydride and carbonyl bridges influence the coupling between the substituents. The X-ray structures of these $60e^-$ clusters have been solved and the adopted solid-state structures are contrasted with the solution NMR data [64]. The molecular structure and ligand fluxionality in $H_4Ru_4(CO)_{11}L$ [where $L = P(C_6F_5)_3$, PMe_2Ph, $P(OMe)_3$, $P(OEt)_3$] have been the focus of a recent report [65]. UV irradiation of the doubly linked dicyclopentadienyl complex [(η^5-$C_5H_3)_2(SiMe_2)_2$]$Ru_2(CO)_4$ under H_2 yields the diruthenium compound [(η^5-$C_5H_3)_2(SiMe_2)_2$]$Ru_2(CO)_4H_2$ and the two tetraruthenium clusters [(η^5-$C_5H_3)_2(SiMe_2)_2]_2Ru_4(CO)_3H_2$ and [(η^5-$C_5H_3)_2(SiMe_2)_2]_2Ru_4(CO)_4H_4$. A linked Cp ligand is required for the formation of these two Ru_4 clusters, as the unlinked Cp derivatives $Cp_2Ru_2(CO)_4$ afford only di- and trinuclear compounds under similar reaction conditions. The X-ray structures of the two Ru_4 products exhibit butterfly and square-planar polyhedral cores, respectively. A detailed mechanism accounting for the wavelength dependence on the product distribution is presented and discussed [66]. New cyclohexadiene-linked tetraosmium clusters have been synthesized. Decarbonylation of $Os_4(CO)_9(RC_2R)(\eta^6$-$C_6H_6)$ (where R = Me, Ph) using Me_3NO in the presence of 1,3- or 1,4-cyclohexadiene furnishes the clusters [$Os_4(CO)_8(RC_2R)(\eta^6$-$C_6H_6)]_2(\mu_2,\eta^2,\eta^2$-$C_6H_8$-1,3) and [$Os_4(CO)_8(RC_2R)(\eta^6$-$C_6H_6)]_2(\mu_2,\eta^2,\eta^2$-$C_6H_8$-1,4), respectively. The X-ray structure of the 2-butyne derivative containing the 1,3-cyclohexadiene link has been solved, making it the first example of two osmium clusters that are joined by a μ_2,η^2,η^2 bridging ligand [67]. Skeletal isomerism in octahedral clusters possessing a M_4E_2 core has been studied by DFT calculations. The energy difference between the two skeletal isomers is dominated by the strength of the E–E bonding. The MO data are discussed relative to the available structural data and to the known properties of $Ru_4Bi_2(CO)_{12}$ and $Os_4Bi_2(CO)_{12}$ [68]. The electronic and magnetic properties of $[Ru_4(\eta^6$-$C_6H_6)_4(\mu_3$-$H)_4]^{2+}$ have been examined by DFT calculations. The small computed energy gap between the diamagnetic singlet state and the paramagnetic triplet state is traced to the absence of a significant Jahn–Teller distortion in the structure of the cluster. The experimentally observed weak paramagnetism is dependent on the nature of the gegenanion [69]. The syntheses, X-ray diffraction structures, and reactivity at tetraosmium clusters possessing μ_2-amido ligands have been published. The amino-substituted clusters $Os_4(\mu$-$H)_4(CO)_{11}(\eta^1$-$NH_2OBu^t)$ and $Os_4(\mu$-$H)_4(CO)_{11}[(\mu$-$H)_3Os(CO)_2(\eta^1$-$NH_2OBu^t)_2Cl]$ have been isolated from the reaction of *O-tert*-butylhydroxylamine hydrochloride with $Os_4(\mu$-$H)_4(CO)_{12}$. Repeating the same reaction in the presence of one equivalent of $Os_3(CO)_{12}$ yields the heptaosmium cluster $[Os_4(\mu$-$H)_4(CO)_{11}(\mu$-$NH_2)][Os_3(\mu$-$H)(CO)_{11}]$, along with the previous osmium clusters. The X-ray structure of the Os_7 cluster exhibits an uncommon polyhedral core, where the Os_4 tetrahedron and the Os_3 triangle are connected by an Os–Os bond. Treatment of $Os_4(\mu$-$H)_4(CO)_{11}(\eta^1$-$NH_2OBu^t)$ with HBr yields a pair of geometric isomers having the formula $Os_4(\mu$-$H)_4(CO)_{11}(\eta^1$-$NH_2)Br$ and structures based on an unsupported butterfly and a supported butterfly frame. These two clusters represent the first examples of μ_2-NH_2 amido Os_4 clusters that serve as models for the adsorption of nitrogen atoms on a stepped metal surface. The thermolysis chemistry of the unsupported butterfly cluster is also reported [70]. A second paper describing the high-yield synthesis of $Os_4(\mu$-$H)_4(CO)_{11}(\eta^1$-$NH_2OBu^t)$ from $Os_4(\mu$-$H)_4(CO)_{12}$ and $^tBuONH_2{\cdot}HCl$ has been published. The cluster product has been allowed to react with HBF_4 in MeCN to furnish the cationic cluster $[Os_4(\mu$-$H)_4(CO)_{11}(\mu$-$NH_2)(MeCN)]^+$. Carrying out the same reaction in the presence of diphenylacetylene gives the geometric isomers $Os_4(\mu$-$H)_2(CO)_{11}(\mu$-$NH_2)[\mu,\eta^3$-Ph(CHC)Ph] and $Os_4(\mu$-$H)_2(CO)_{11}(\mu$-$NH_2)[\eta^1$-Ph(CH=CPh)]. Carbonylation of the cationic acetonitrile-bound cluster in $CHCl_3$ gives the neutral clusters $Os_3(\mu$-$H)_2(CO)_9(\mu$-$NH_2)Cl$ and $Os_4(\mu$-$H)_3(CO)_{12}(\mu$-$NH_2)$. Thermolysis of this latter cluster produces the nitrene-capped cluster $Os_4(\mu$-$H)_3(CO)_{12}(\mu_3$-NH), which represents the first structurally characterized tetraosmium nitrene-containing cluster. Seven X-ray structures have been solved, and the correlation between the ^1H NMR chemical shifts and the structural geometry is discussed [71]. The activation of tri(2-furyl)phosphine by $Ru_4(\mu$-$H)_4(CO)_{12}$ in refluxing THF proceeds readily to produce an isomeric pair of clusters having the formula $Ru_4(\mu$-$H)_4(CO)_{10}(PFu_3)_2$, the μ-phosphido cluster $Ru_4(\mu$-$H)_2(CO)_8(PFu_3)_2(\mu$-$PFu_2)(\mu,\eta^1,\eta^2$-$C_4H_3O)$, and the μ_3- and μ_4-phosphinidene-capped clusters $Ru_4(\mu$-$H)_2(CO)_{12-x}(PFu_3)_x(\mu_3$-PFu) (where $x = 0, 2, 3$) and $Ru_4(\mu$-$H)_2(CO)_9(PFu_3)_2(\mu_4$-$PFu)(\mu_3,\eta^1,\eta^1,\eta^2$-$C_4H_2O)$. The X-ray structure of $Ru_4(\mu$-$H)_2(CO)_{12}(\mu_3$-PFu) is shown in Fig. 7. The ability of the PFu_3 ligand to serve as a source of furyne, furyl, phosphide, and phosphinidene fragments on tetrametallic frameworks is fully outlined. The redox behavior and molecular orbital calculations on these metallophosphorus clusters have been explored as a function of the coordination modes exhibited by the phosphorus-containing moieties [72].

New germanium-rich pentaruthenium carbide clusters have been prepared from $Ru_5(CO)_{15}(\mu_5$-C) and Ph_3GeH upon thermolysis at 150 °C. The major products isolated were $Ru_5(CO)_{11}(\mu$-CO)$(\mu$-$GePh_2)_3(\mu_5$-C) and $Ru_5(CO)_{11}(\mu$-$GePh_2)_4(\mu_5$-C), whose solid-state structures reveal the presence of a square pyramidal Ru_5 core with $GePh_2$ moieties bridging three and four edges of the Ru_5 square base, respectively. The latter product loses CO at 150 °C and reacts with added H_2 to give $Ru_5(CO)_{10}(\mu$-$GePh_2)_2(\mu_3$-$GePh)_2(\mu_3$-$H)(\mu_4$-CH) ultimately. The conversion of the carbide moiety into a methylidyne ligand and the reactivity of the ancillary

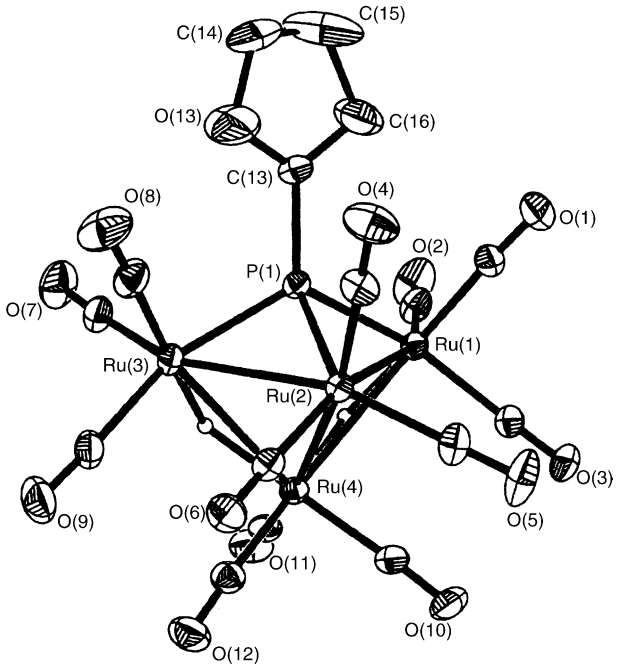

Fig. 7. X-ray structure of $Ru_4(\mu\text{-}H)_2(CO)_{12}(\mu_3\text{-}PFu)$. Reprinted with permission from Organometallics. Copyright 2003 American Chemical Society.

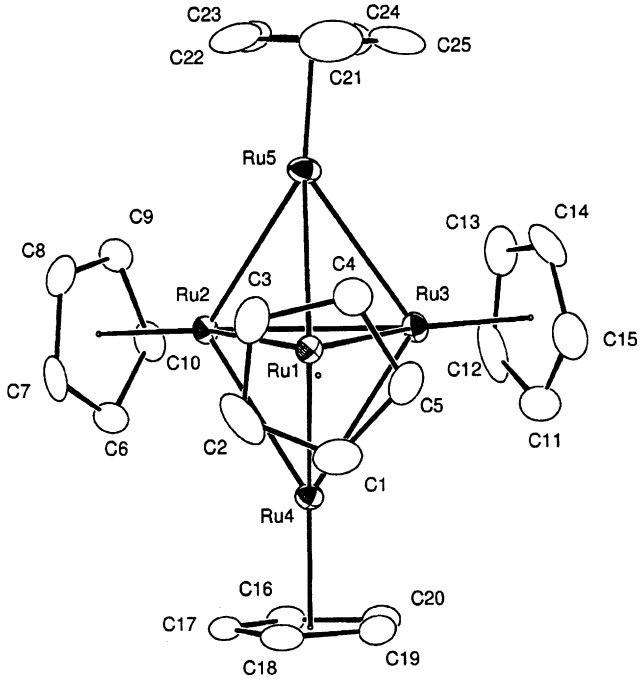

Fig. 8. X-ray structure of $Cp_5Ru_5H_7$. Reprinted with permission from Organometallics. Copyright 2003 American Chemical Society.

$GePh_2$ ligands in benzene elimination schemes are discussed. All new clusters have been fully characterized in solution by IR and NMR spectroscopies, and in the solid state by X-ray crystallography [73]. A new gas sensor based on an ArgoGel resin supported with a phosphinated $Ru_5(CO)_{15}(\mu_5\text{-}C)$ cluster has been described. The cluster-containing beads reveal a definitive color change upon treatment with H_2S, SO_2, or CO. The observed FT-IR spectral changes are related to polyhedral changes in the cluster core as a result of ligand addition [74]. The ruthenium diamine complex CpRu(tmeda)Cl reacts with $LiAlH_4$ to give the pentaruthenium cluster $Cp_5Ru_5H_7$, whose X-ray structure (Fig. 8) exhibits a five-vertex *closo* polyhedron. The related mixed-ligand cluster $Cp_4Cp^*Ru_5H_7$ has also been synthesized, and the fluxional behavior of the exchanging CpRu groups have been probed by VT ^1H NMR spectroscopy. Plausible mechanisms for the axial/equatorial exchange of the CpRu groups are outlined and discussed. The Cp_5Ru_5 cluster reacts with $PhPH_2$ at room temperature to produce the six-vertex *closo* cluster $H_5(CpRu)_5PPh$. This new phosphinidene-capped cluster was characterized in solution by IR and NMR measurements [75].

A report describing the analysis of organometallic cluster compounds using ion trap mass spectrometry has appeared. Some of the examples highlighted include spectral data for $Ru_6(CO)_{17}(\mu_6\text{-}C)$ in MeOH/MeO^-, $[CoRu_3(CO)_{13}]^-$, and $[HOs_3W(CO)_{14}]^-$ [76]. Refluxing $Os_3(CO)_{11}(MeCN)$ in octane and in the presence of oxygen furnishes the hexaosmium cluster $Os_6(CO)_{16}(\mu_4\text{-}O)(\mu\text{-}OH)_2(\mu\text{-}CO)_2$, which when subjected to vacuum pyrolysis gives $Os_{12}(CO)_{30}$. This is the highest nuclearity neutral binary osmium cluster isolated and structurally characterized to date. The Os_6 cluster contains 94 valence electrons, treating the μ_4-oxo moiety as a $4e^-$ donor ligand. This electron count represents two electrons in excess of the theoretically expected number of 92 cluster valence electron and is acceptable given the boat structure adopted by the Os_6 frame. The two extra electrons occupy an antibonding orbital associated with the tetraosmium metal plane, leading to a weakening of the Os–Os bonds within the square base. DFT calculations support this contention as do the data obtained from cyclic voltammetry and controlled potential coulometric experiments. The Os_{12} cluster possesses 156 valence electrons, consistent with the EAN rule. The Os_{12} polyhedron is irregular, insomuch as it does not conform to the normal geometries found in other dodecanuclear clusters of Pd, Ir, and Rh. There is a distorted central square pyramid containing five osmium atoms that are fused with three tetrahedra via edge sharing and that are capped by one osmium atom. The remaining osmium center face caps one of the triangular faces of the internal Os_5 pyramid [77]. The VT ^1H NMR data and X-ray diffraction structure of $[H_5Os_{10}(CO)_{24}]^-$ have been reported. This high nuclearity cluster is obtained in high yield through hydrogenation of the silica-supported compound $[Os(CO)_3(OH)_2]_n$ at 200 °C. The VT NMR data reveal that the μ_2- and μ_3-hydrides exchange via a facile edge-shift process with exchange among the μ_3-hydrides being more difficult. The exchange pathways were also investigated by using ^1H 2D EXSY measurements. Hydride exchange schemes and comparisons to related hydride-bridged clusters are discussed [78].

2.4. Group 9 clusters

No dealkylation of the alkyl group associated with the carbyne carbon in the clusters $[Cp_3Co_3(\mu_3\text{-}S)(\mu_3\text{-}CSR)]^+$ (where R = Me, Et) was observed when these clusters were treated with $[PhCH_2NMe_3][OH]$, NaOH, NaOMe, or NaOEt. The mixed-metal cluster $[(CpCo)_2\{Fe(CO)_2PPh_3\}(\mu_3\text{-}S)(\mu_3\text{-}CSMe)]^+$ exhibits nucleophilic attack at a CO ligand when treated with the same oxygen-based anionic reagents. The reversible formation of $[(CpCo)_2\{Fe(CO)(CONu)PPh_3\}(\mu_3\text{-}S)(\mu_3\text{-}CSMe)]$ was demonstrated by spectroscopic measurements, coupled with the regeneration of the starting cluster upon treatment with aqueous acids. The X-ray structure of $[Cp_3Co_3(\mu_3\text{-}S)(\mu_3\text{-}CSMe)]^+$ has been solved, and the bonding parameters between the Co_3S and the CS fragments have provided insight into the lack of reactivity of the thiomethyl group in the cluster. The cationic charge in these clusters is not localized on the μ_3-CSR moiety but rather on the cluster core [79]. A paper describing the transformations of organoarsine-oxides to organoarsine-sulfides at di- and tricobalt compounds has appeared. The arsine-bridged clusters $RCCo_3(CO)_7[\mu\text{-}(AsMe_2)_2O]$ (where R = Me, Cl) react with added H_2S with elimination of H_2O to give $RCCo_3(CO)_7[\mu\text{-}(AsMe_2)_2S]$. This process is reversible depending upon the reaction conditions. The direct reaction of $RCCo_3(CO)_9$ with $(AsPh_2)_2S$ affords the corresponding diarsine-bridged cluster $RCCo_3(CO)_7[\mu\text{-}(AsPh_2)_2S]$ in moderate yield. Thermolysis of $ClCCo_3(CO)_7[\mu\text{-}(AsPh_2)_2S]$ produces the sulfido-capped cluster $Co_3(CO)_7(\mu_3\text{-}S)[\mu\text{-}(AsPh_2)_2O](\mu\text{-}AsPh_2S)$ in low yield. Four X-ray structures have been solved and their important structural features are discussed relative to the proposed reaction mechanism [80]. The sulfido-capped cluster $Co_3(CO)_7(\mu_3\text{-}S)(\mu\text{-}S,P\text{-}SPMe_2)$ has been allowed to react with Ph_2Ppy in THF at 90 °C to afford $Co_3(CO)_5(\mu_3\text{-}S)(\mu\text{-}S,P\text{-}SPMe_2)(\mu\text{-}P,N\text{-}Ph_2Ppy)$ and $Co_3(CO)_4(\mu_3\text{-}S)(\mu\text{-}S,P\text{-}SPMe_2)(\mu\text{-}P,N\text{-}Ph_2Ppy)(Ph_2Ppy)$. Both new clusters were characterized in solution and by X-ray crystallography. The diphosphine ligands dppm and dppe have also been examined for their reactivity with the cluster $Co_3(CO)_7(\mu_3\text{-}S)(\mu\text{-}C,N\text{-}C_5H_4N)$. Here the major products isolated are $Co_3(CO)_5(\mu_3\text{-}S)(\mu\text{-}C,N\text{-}C_5H_4N)(\mu\text{-}P\text{–}P)$ and $Co_3(CO)_5(\mu_3\text{-}S)[\mu\text{-}C(O),\ N\text{-}C_5H_4N(C{=}O)](\mu\text{-}P\text{–}P)$. The carbonylation occurring at the Co-C(pyridyl) bond in the products was ascertained by X-ray crystallography [81]. The thermolysis chemistry of $CpCo(PPh_3)(\eta^2\text{-dmad})$ has been revisited. Besides the *ortho*-metalated vinyl-phosphonium compound $CpCo[\eta^2\text{-}(MeO_2C)CH{=}C(CO_2Me)PPh_2(\eta^1\text{-}o\text{-}C_6H_4)]$, which represents the major product of the reaction, the tricobalt cluster $Cp_3Co_3[\mu_3,\eta^3\text{-}C(CO_2Me)]_2$ has been obtained in low yield. The X-ray structure of the bis(carbyne) cluster accompanies this report [82]. A new approach to the synthesis of Co_3 clusters that are linked by carbon chains has been published. The reaction between $Co_3(\mu_3\text{-}CBr)(CO)_7(\mu\text{-dppm})$ and $[Au\{P(tol)_3\}]_2[\mu\text{-}(C_2)_n]$ (where $n = 2$–4) gives the new cobalt-linked clusters $[Co_3(CO)_7(\mu\text{-dppm})]_2[\mu_3{:}\mu_3\text{-}C(C_2)_nC]$. Insertion of TCNE into the unsaturated carbon chain of the tris(alkyne) occurs readily to furnish $[Co_3(CO)_7(\mu\text{-dppm})]_2[\mu_3{:}\mu_3\text{-}C(C_2)_2C\{{=}C(CN)_2\}C\{{=}C(CN)_2\}C]$, whose X-ray structure confirms the nature of the insertion product [83]. The reaction between $Me_2NC_6H_4SiH_3$ and $Co_2(CO)_8$ proceeds unexpectedly to give the cluster compound $Me_2NC_6H_4Si[Co(CO)_4][OCCo_3(CO)_9]_2$. X-ray diffraction analysis reveals that the silicon atom coordinates the two $-OCCo_3(CO)_9$ groups via the oxygen atom. Parallels between this compound and other systems that bind the $-OCCo_3(CO)_9$ moiety are discussed [84]. The reaction chemistry of the incomplete cubane-type sulfido-hydrosulfido cluster $[Cp^*_3Ir_3(\mu_3\text{-}S)(\mu_2\text{-}SH)_3]^+$ with $SbCl_3$, $SbCl_5$, $BiCl_3$, and $Pd(PPh_3)_4$ has been investigated [85]. The benzylidyne-capped cluster $PhCCo_3(CO)_9$ reacts with the diphosphine ligand 2,3-bis(diphenylphosphino)maleic acid-thioanhydride (bmata) to initially afford $PhCCo_3(CO)_7$(bmata). CO loss, followed by P–C bond cleavage and reductive coupling with the benzylidyne moiety, produces $Co_3(CO)_6[\mu_2,\eta^2,\eta^1\text{-}C(Ph)C{=}C(PPh_2)C(O)SC(O)](\mu_2\text{-}PPh_2)$. The molecular structure of the phosphido cluster confirms the reaction sequence. These results are discussed relative to the similar bma- and bpcd-substituted clusters. The cyclic voltammetric behavior of the new phosphido-bridged cluster was also studied [86]. The synthesis of the benzylidyne-capped trirhodium and cobalt-rhodium clusters $M_3Cp_3(\mu_3\text{-}CPh)_2$ (where $M_3 = Rh_3$, $CoRh_2$, Co_2Rh) from $CpRh(CO)_2$, $CpCo(CO)_2$, and diphenylacetylene has been reported. The solid-state structures of all three clusters have been determined and are discussed with respect to $Co_3Cp_3(\mu_3\text{-}CPh)_2$. The redox trends as a function of the number of rhodium atoms present in the cluster and the results of DFT calculations are discussed [87]. Carbynyl-tricobalt cluster transformations have been examined by synthetic and NMR methods. Prolonged thermolysis of the terminal alkyne compound (2-*endo*-ethynylborneol)$Co_2(CO)_6$ in acetone solvent gives the tricobalt clusters (2-norbornylidene)$CHCCo_3(CO)_9$ and [2-(2-hydroxylbornyl)]$CH_2CCo_3(CO)_9$, as shown in Fig. 9 for the latter product. Mechanistic pathways accounting for the formation of $RCH_2CCo_3(CO)_9$ clusters upon protonation of the alkyne compounds $(RC_2H)Co_2(CO)_6$ are presented and fully discussed [88].

The associative rate constants for P-ligand substitution in $Rh_4(CO)_{12}$ have been analyzed qualitatively for their steric and electronic properties of the incoming nucleophile by the QALE method. These data have allowed for the evaluation of the "aryl effect" and the importance of π-acidity of the phosphite nucleophiles in the substitution reactions. The utility of graphical analysis by the construction of a three-dimensional "$\log k_2$ surface" is fully described [89]. The synergism exhibited by $Rh_4(CO)_{12}/HMn(CO)_5$ in the hydroformylation of alkenes has been studied by using in situ FT-IR spectroscopy. The kinetic data reveal the existence of a linear-bilinear rate law where the reaction rate

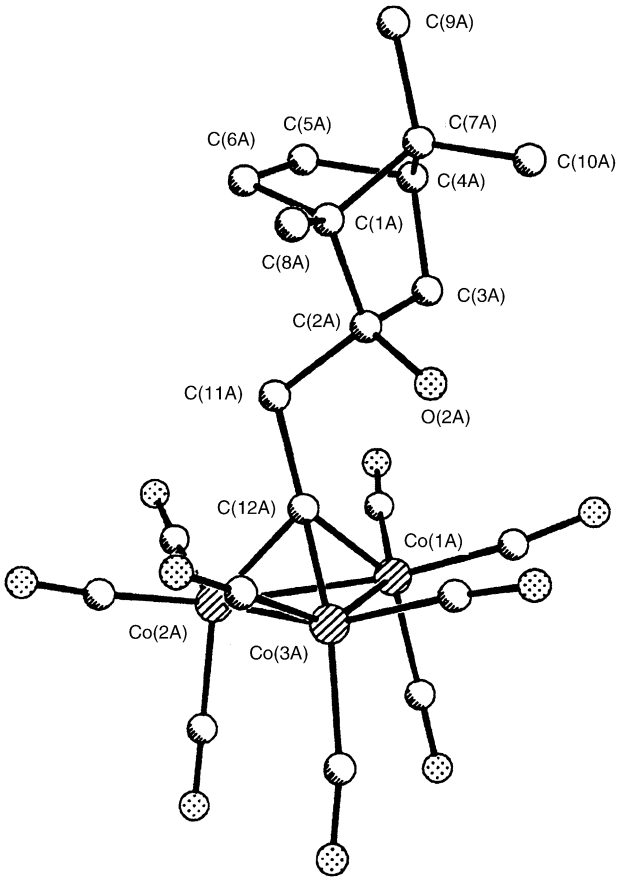

Fig. 9. X-ray structure of [2-(2-hydroxylbornyl)]$CH_2CCo_3(CO)_9$. Reprinted with permission from Organometallics. Copyright 2003 American Chemical Society.

is proportional to $[RCORh(CO)_4][CO]^-[H_2]$ (classical rate) and $[RCORh(CO)_4][HMn(CO)_5][CO]^-$ (synergistic rate). In terms of the latter expression, evidence is presented for a hydride attack on the acyl intermediate, which rules out cluster catalysis and underscores the importance of the bimetallic catalytic binuclear elimination sequence. The detailed catalytic mechanism that accompanies this work is fully discussed [90]. The charge density in $Co_4(CO)_{12}$, $Co_2(CO)_8$, and $Co_2(CO)_6(InMe_2)_2$ has been analyzed by using the theory of atoms in molecules (AIM) method. The advantages of using charge densities in bonding analyses are described [91]. The synthesis, X-ray structure, and fluxional behavior of $Rh_4(CO)_6(\mu\text{-}Me_2PCH_2PMe_2)_3$ have been published. Treatment of $Rh_4(CO)_{12}$ with three equivalents of $Me_2PCH_2PMe_2$ at room temperature produces the title product. All three diphosphine ligands bridge adjacent rhodium centers associated with one of the four triangular faces of this *nido* cluster. The fluxional process involving carbonyl site exchange that scrambles one μ_2-CO with one η^1-CO and that leaves an imbalance in the formal electron count at two rhodium centers is discussed. The ^{103}Rh, ^{31}P, and ^{13}C NMR data are presented and used in the discussion of the proposed exchange mechanism [92]. Insertion of $SnBr_2$ into the Ir–Br bond of $[Ir_4(CO)_{11}Br]^-$ yields $[Ir_4(CO)_{11}(SnBr_3)]^-$ in good yield. Treatment of $[Ir_4(CO)_{11}Br]^-$ with $[SnCl_3]^-$ in THF affords $[Ir_4(CO)_{11}(SnCl_3)]^-$ and $[Ir_4(CO)_{10}(SnCl_3)_2]^-$ depending on the stoichiometry of $[SnCl_3]^-$ employed. The reaction of $Ir_6(CO)_{16}$ with $[SnCl_3]^-$ in refluxing THF produces $[Ir_6(CO)_{15}(SnCl_3)]^-$. One of the two $SnCl_3$ ligands in $[Ir_4(CO)_{10}(SnCl_3)_2]^-$ functions as a one-electron donor ligand and is terminally bound to one of the iridium centers, and in $[Ir_4(CO)_{11}(SnCl_3)]^-$ the lone $SnCl_3$ ligand serves as an edge-bridging ligand. The $SnCl_3$ ligand in the hexairidium cluster caps one of the triangular Ir_3 faces, as shown by X-ray diffraction analysis. The Ir–Sn bond length trends as a function of the coordination mode displayed by the $SnCl_3$ ligand are described [93]. The tetracobalt cluster $Co_4(CO)_7(\mu\text{-}CO)_3[\mu_3\text{-}P(tmp)]$ has been obtained from the reaction of $Co_2(CO)_8$ with the terminal chloroaminophosphido complexes $Cp^*Ru(CO)_2[P(Cl)tmp]$ and $CpRu(CO)_2[P(Cl)tmp]$. Use of the chloroaminophosphido complex $Cp^*Ru(CO)_2[P(Cl)NPr^i_2]$ in the reaction with $Co_2(CO)_8$ furnishes the spiked-triangular cluster $Cp^*RuCo_3(CO)_8(\mu\text{-}CO)_2(\mu_3\text{-}PNPr^i_2)$, whose X-ray structure confirms that the Cp^*Ru moiety is retained in the product cluster. Whereas the reaction between the molybdenum phosphido complex $CpMo(CO)_2[P(Cl)tmp]$ and $Co_2(CO)_8$ gives the aforementioned Co_4 cluster, the reaction employing $Cp^*Mo(CO)_3[P(Cl)NPr^i_2]$ yields the mixed-metal tetrahedral cluster $Cp^*MoCo_3(CO)_5(\mu\text{-}CO)_4(\mu_3\text{-}PNPr^i_2)$ as the major product. Three X-ray structures and reaction schemes accompany this report [94]. CO ligand substitution in $Co_4(CO)_{11}(\mu_4\text{-}SiC_6H_4R)_2$ (where R = H, OMe, NMe_2) by isonitriles has been examined. The various isonitrile-substitution products have been subjected to study by electrospray mass spectrometry, providing evidence for the replacement of up to nine CO groups. The molecular structure of the tetrasubstituted cluster $Co_4(CO)_7(xyNC)_4(\mu_4\text{-}SiC_6H_4OMe)_2$ has been crystallographically determined and discussed relative to other Co_4E_2 cluster compounds [95]. Thermolysis of $Ir_4(CO)_{12}$, H_2, and PPh_3 at 90 °C in toluene solvent affords the hydride cluster $Ir_4H_8(CO)_4(PPh_3)_4$ in high yield. Solution IR and NMR measurements and X-ray crystallography reveal that each iridium center is substituted by a PPh_3 ligand and one terminal hydride group. The remaining four hydride ligands bridge Ir–Ir bonds in the cluster. Two isomeric forms of the product cluster exist in solution, on the basis of ^1H and ^{31}P NMR data [96]. The stabilization of cluster polyhedra through the use of short-bite angle ligands has been described. The coordination of the ligands dppm, dppa, and dppaSi to $Co_4(CO)_{12}$, followed by alkyne insertion reactions, has been studied. Analogous substitution chemistry using $Si(OR)_3$-functionalized alkynes has allowed for the synthesis of Co_4 clusters that could be employed in sol–gel processes [97].

The one-pot catalytic hydroformylation-cyclotrimerization of cyclopentene and cyclohexene to 2,4,6-trisubstituted-1,3,5-trioxanes has been confirmed. The catalytic system is comprised of $Rh_6(CO)_{16}$ and $H_3PW_{12}O_{40}\cdot xH_2O$ using THF and syngas [98]. The photoassisted transfer hydro-

genation and thermal hydrogenation of norbornadiene and quadricyclane using $Rh_6(CO)_{16}$ have been described [99]. The synthesis and chemical properties of the hexairidium chain complex HH, HT, HH-$Ir_6(\mu\text{-}OPy)_6I_2(CO)_{12}$ have been published. The complex contains an unprecedented linear metal chain where the iridium center exhibits a formal oxidation state of +1.33. Stepwise degradation of this Ir_6 complex has afforded the three individual Ir_2 moieties that comprised the original Ir_6 entity, allowing for the configuration of each Ir_2 link to be established. The X-ray structures for the Ir_6 and the HH-$Ir_2(\mu\text{-}OPy)_2I_2(CO)_4$ complexes have been solved [100]. The solution structure and fluxional behavior of $Rh_6(CO)_{14}(\mu,\eta^2\text{-dppm})$, $Rh_6(CO)_{14}(\mu,\eta^2\text{-dppe})$, and $Rh_6(CO)_{14}(\mu,\eta^2\text{-dppef})$ have been investigated by using various NMR techniques. The NMR data are contrasted with the observed solid-state structure of each cluster. The ethano bridge in the latter Rh_6 clusters exhibit two enantiomeric forms of the cluster due to a rocking motion of the bridging diphosphine ligands. The exchange rate measured is shown to depend on the non-bonding van der Waal's interactions between the substituents on the phosphorus groups and the neighboring CO groups. The lower exchange rates measured for $Rh_6(CO)_{14}(\mu,\eta^2\text{-dppef})$ are attributed to the steric requirements of the fluorinated phenyl rings that hinder the racemization process [101]. The solution structures and dynamic ligand behavior found for $Rh_6(CO)_{14}(\mu\text{-PX})$ [where PX = diphenyl(2-pyridyl)phosphine, diphenyl(2-thienyl)phosphine, diphenylvinylphosphine] have been studied by multinuclear NMR spectroscopy and X-ray crystallography in the case of the latter phosphine ligand. The multiple localized CO-exchange pathways and their mechanisms are outlined. The vinyl moiety in $Rh_6(CO)_{14}(\mu,\kappa^3\text{-}Ph_2PCH{=}CH_2)$ is hemilabile and displays facile reorientation behavior [102]. The syntheses and X-ray structures of hexarhodium clusters containing heterobidentate phosphine ligands have appeared. Clusters of the form $Rh_6(CO)_{14}(\mu,\kappa^3\text{-PX})$ have been prepared from $Rh_6(CO)_{16-x}(MeCN)_x$ (where $x = 1$, 2) and the phosphine ligands diphenyl(benzothienyl)phosphine, diphenyl(2-thienyl)phosphine, di(2-thienyl)phenylphosphine, tris(2-thienyl)phosphine, diphenyl(2-pyridyl)phosphine, and diphenylvinylphosphine. The kinetics for the formation of the bridged Rh_6 clusters from the corresponding monosubstituted $Rh_6(CO)_{15}(\kappa^1\text{-PX})$ clusters are reported. The ligand tris(2-furyl)phosphine in $Rh_6(CO)_{15}[\kappa^1\text{-P(2-furyl)}_3]$ shows no evidence for the formation of $Rh_6(CO)_{14}[\mu,\kappa^3\text{-P(2-furyl)}_3]$ and reveals that the ancillary phosphine cannot bridge adjacent rhodium centers by oxygen and phosphorus coordination. The X-ray structures of five clusters accompany this paper [103].

The synthesis and structural characterization of $[Co_{10}P_2(CO)_{23}H]^{2-}$ have been published. This decacobalt cluster was isolated from the reaction of $[Co_6(CO)_{15}]^{2-}$, $[Co(CO)_4]^-$, and PBr_3 in THF. The presence of two partially encapsulated phosphorus atoms was verified by X-ray crystallography. The redox properties and temperature-dependent magnetic susceptibility have been examined, and the data support the existence on one unpaired electron that is delocalized over the cluster frame [104]. Treatment of $Rh_6(CO)_{16}$ with excess cycloheptatriene in refluxing toluene initially gives $Rh_6(CO)_{13}(C_7H_8)$, followed by conversion to $Rh_{11}(CO)_{14}(C_7H_7)_3$. The X-ray structure of the Rh_{11} cluster consists of a trioctahedral metal cage that possesses a condensed common edge. The three $\mu_3,\eta^2,\eta^2,\eta^2$-bound cycloheptatrienyl ligands are equivalent and reside on the top of the triangular Rh_3 faces [105].

2.5. Group 10 clusters

The use of $[Pt_3(\mu\text{-}PBu^t_2)_3L(X)]^{n+}$ and $[Pt_6(\mu\text{-}PBu^t_2)_4(CO)_4X_2]^{2n+}$ in the construction of covalently linked platinum dendrimers that are connected by σ-alkenyl spaces has been reported [106]. The stoichiometric and catalytic activation of the bromine group in α- and β-2,3,4-tri-*o*-acetyl-5-thioxylopyranosyl bromide (Xyl-Br) inside the cavity of $[Pd_3(dppm)_3(CO)]^{2+}$ has been achieved. Here the initial step involves abstraction of a bromine atom from the pyranosyl bromide to form a $Pd_3(Br)^+$ species. The catalytic activation sequence is triggered by the $2e^-$ reduction of the $Pd_3(Br)^+$ adducts to generate a $Pd_3{}^0$ species that is able to associatively react with the pyranosyl bromide via a $Pd_3{}^{2+}\cdots$Xyl-Br host–guest assembly. The involvement of the radical species $Xyl^\bullet$ in these reactions is confirmed by spin trapping studies using TEMPO and DMPO [107]. The activation of alkyl halides and acid halides using the unsaturated cluster $[Pd_3(dppm)_3(CO)]^{2+}$ has been presented. The involvement of a paramagnetic Pd_3 species is outlined and supported by electrochemical analyses [108]. The reaction of $[(C_6F_5)_2Pt(\mu\text{-}PPh_2)Pt(\mu\text{-}PPh_2)Pt(C_6F_5)_2]^{2-}$ with *cis*-$Pt(C_6F_5)_2(THF)_2$ (1:2 ratio) gives the dinuclear complex $[Pt_2(\mu\text{-}C_6F_5)_2(C_6F_5)_4]^{2-}$ and the tetraplatinum compound $[Pt_4(\mu\text{-}PPh_2)_4(C_6F_5)_5]^-$. The molecular structure of the latter compound reveals the presence of two Pt–Pt bonds and an unusual $\mu\text{-}PPh_2$ ligand that is bound to one of the platinum centers via an η^2-phenyl interaction. The Pt_4 complex reacts with $HClO_4$ to give the neutral cluster $Pt_4(\mu\text{-}PPh_2)_4(C_6F_5)_5$, which contains three Pt–Pt bonds and a $\mu_3\text{-}PPh_2$ moiety. This neutral cluster readily reacts with donor ligands to yield $Pt_4(\mu\text{-}PPh_2)_4(C_6F_5)_5L$ (where L = PPh_3, pyridine) [109]. The novel perylene compounds $[Pd_4(\mu,\eta^2,\eta^2,\eta^2,\eta^2\text{-perylene})_2L_2]^{2+}$ (where L = MeCN, pyridine) have been synthesized and structurally characterized in the case of the MeCN derivative (Fig. 10). This represents the first example of a polynuclear aromatic hydrocarbon ligand that can support a metal–metal bond chain. The perylene ligands are replaced by 1,8-diphenyl-1,2,5,7-tetraene at room temperature in CD_2Cl_2 solvent [110].

A report that demonstrates the construction of one-dimensional platinum clusters has appeared. Here the coupling of $Pt_6(CO)_4(\mu\text{-}PBu^t_2)_4(CC{-}C_6H_4{-}CCH)_2$ with $Pt_3(\mu\text{-}PBu^t_2)_3(CO)_2Cl$ using CuI/amine synthetic coupling

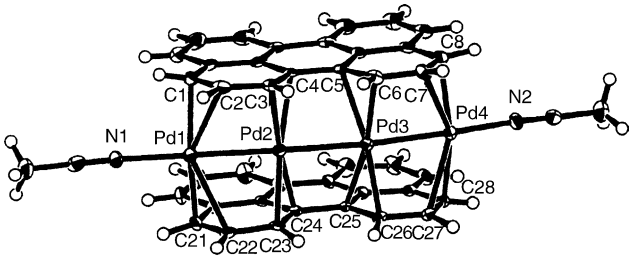

Fig. 10. X-ray structure of $[Pd_4(\mu,\eta^2,\eta^2,\eta^2,\eta^2\text{-perylene})_2(MeCN)_2]^{2+}$. Reprinted with permission from Journal of the American Chemical Society. Copyright 2003 American Chemical Society.

methods gives the air-stable cluster $Pt_6(CO)_4(\mu\text{-}PBu^t_2)_4[CC{-}C_6H_4{-}CC\{Pt_3(\mu\text{-}PBu^t_2)_3(CO)_2\}]_2$. The central Pt_6 portion of the molecule is separated from the two Pt_3 cluster units by conjugated 1,4-diethynylphenyl groups [111]. The isostructural Tl(I) sandwich compounds $[(\mu_6\text{-}Tl)Pt_6(\mu_2\text{-}CO)_6(PEt_3)_6]^+$ and $[(\mu_6\text{-}Tl)Pd_6(\mu_2\text{-}CO)_6(PEt_3)_6]^+$ have been synthesized and structurally characterized. Each compound exhibits a M_3TlM_3 sandwich structure that is held together by delocalized electrostatic M_3–Tl–M_3 bonding. The greater kinetic lability of the Pd analogue is revealed by its conversion to the known cluster $[Tl_2Pd_{12}(\mu_2\text{-}CO)_6(\mu_3\text{-}CO)_3(PEt_3)_9]^{2+}$ [112]. A new and active hydrogenation catalyst formed from the attachment of $[Pt_{12}(CO)_{24}]^{2-}$ to the surface of functionalized fumed silica has been described. The grafted cluster has been characterized by normal spectroscopic methods, and its activity in ketone and nitrile hydrogenation reactions is discussed [113]. ^{31}P NMR data are reported that conclusively prove the interconversion between $Pd_{23}(CO)_{20}(PEt_3)_{10}$ and $Pd_{23}(CO)_{20}(PEt_3)_8$. A structural diagram that outlines a plausible reaction scenario is presented and discussed. The structural changes attendant in this reaction are discussed with respect to the abnormal capacity of ligated palladium clusters to experience significant changes in their metal-core geometries upon ligand addition or removal [114]. The generation of nanosized Pd_{30}- and Pd_{54}-core geometries possessing cuboctahedral-based metal polyhedra is described. Deligation of $Pd_{10}(CO)_{12}(PEt_3)_6$ under CO furnishes the new clusters $Pd_{30}(CO)_{26}(PEt_3)_{10}$ and $Pd_{54}(CO)_{40}(PEt_3)_{14}$, along with the known cluster compound $Pd_{38}(CO)_{28}(PEt_3)_{12}$. The solid-state structures of these new clusters were established by X-ray crystallography [115].

2.6. Group 11 clusters

The homoleptic tetranuclear compound $[Cu(C_6F_5)]_4(\eta^2\text{-toluene})_2$ has been synthesized from pentafluorophenylcopper and toluene. The coordination of the two toluene molecules leads to a structural change from the normally observed square planar $[Cu(C_6F_5)]_4$ core to a distorted butterfly structure. The tetracopper core is disrupted in the presence of donor solvents such as MeCN and DMSO [116]. The synthesis and structural characterization of a tetranuclear silver cluster that is stabilized by a mixed-donor N-heterocyclic carbene macrocycle have been reported. The pyridine–pyrrole carbene linked cyclophane ligand employed in this study is exceptional in its ability to stabilize silver clusters [117].

3. Heterometallic clusters

3.1. Trinuclear clusters

The reactivity of the early-late cluster $CpTi(acac)(\mu_3\text{-}S)_2Ir_2(CO)_4$ towards electrophiles has been studied. Iodine reacts with the title cluster to furnish $CpTi(acac)(\mu_3\text{-}S)_2Ir_2I_2(CO)_4$. This diiridium(II) cluster actually consists as an isomeric mixture with respect to the relative positions of the iridium-bound iodo ligands. Iodoalkanes react with the parent cluster cleanly and stereoselectively to afford a single isomer of $CpTi(acac)(\mu_3\text{-}S)_2Ir_2(R)(I)(CO)_4$, where a carbonyl and iodo ligand are situated *trans* across the iridium–iridium bond. The X-ray structure of $CpTi(acac)(\mu_3\text{-}S)_2Ir_2(CHI_2)(I)(CO)_4$ (Fig. 11) confirms the stereochemical outcome associated with this oxidative addition reaction. Treatment of the parent cluster with activated acetylenes leads to clusters possessing a *cis*-metalated alkene ligand. The two products, which have the general formula $CpTi(acac)(\mu_3\text{-}S)_2Ir_2(CO)_4(\mu,\eta^1\text{-}RC_2CO_2Me)$ (where R = H, CO_2Me), have been characterized in solution and the data support a *cis*-metalated alkene moiety by coordination across the Ir–Ir vector [118].

The synthesis and structural characterization of the chalcogenide clusters $[E_2Cr_2Fe(CO)_{10}]^{2-}$ (where E = Se, Te) have been reported. Treatment of a mixture of $Cr(CO)_6$ and $Fe(CO)_5$ in the presence of concentrated KOH/MeOH with Te or Se powder affords the title clusters, which have been isolated as the [PPN] salts. Each cluster exhibits

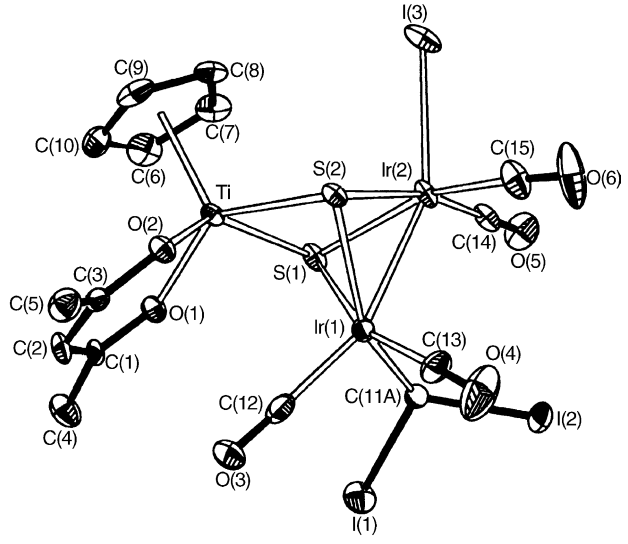

Fig. 11. X-ray structure of $CpTi(acac)(\mu_3\text{-}S)_2Ir_2(CHI_2)(I)(CO)_4$. Reprinted with permission from Inorganic Chemistry. Copyright 2003 American Chemical Society.

a distorted E_2Cr_2Fe trigonal bipyramidal core. These 50-electron clusters are electron rich and do not obey PSEP theory in terms of the adopted five-vertex *closo* polyhedra found by X-ray crystallography. SQUID magnetic susceptibility data reveal that both clusters are highly paramagnetic with an effective magnetic moment (μ_{eff}) of 4.80μ_B (Te) and 5.38μ_B (Se) at room temperature [119]. The reaction of metallophosphanide anions with selected metal halides (MlnX) has been shown to yield a variety of di, tri, and tetranuclear compounds. Some of the new cluster compounds that have been isolated and structurally characterized include $(OC)_6CpCoMnMo(\mu\text{-}CO)(\mu\text{-}PPh_2)[\mu_3,\eta^2(||)\text{-dmad}]$, $Os_3(CO)_{10}FeCp(CO)(\mu\text{-}PPh_2)(\mu\text{-}CO)$, and $Os_3(CO)_{10}(\mu\text{-}PPh_2)(\mu\text{-}MPR_3)$ (where M = Au, R = Ph; M = Ag, R = Me). The former Os_3Fe cluster contains an Os_3 triangle with a pendant Fe "spiked" atom, while the latter Os_3M clusters exhibit butterfly polyhedral cores [120]. The double-star shaped cluster $Cp_2MoFe_2(\mu_3\text{-}S)_2(CO)_6$ has been obtained from the reaction of $Fe_2(CO)_6(\mu_2\text{-}S_2)$ with Cp_2MoH_2. The $MoFe_2$ cluster and the related tetranuclear cluster $Cp_2Mo_2Fe_2(\mu_3\text{-}S)_2(CO)_8$ have been employed as OMCVD precursors for the fabrication of mixed-metal oxide films on silica and borosilicate glass substrates. XRD analysis confirmed the film composition as $Fe_2Mo_xO_x$ ($3 < x 4$), while the film morphology was also studied through the use of XPS and SEM techniques [121]. The reaction of $CpMoMn(CO)_8$ and elemental selenium in the presence of Me_3NO and room light produces the tetranuclear cluster $Cp_2Mo_2Mn_2(CO)_7(\mu_3\text{-}Se)_4$ (major) and $CpMoMn(CO)_5(\mu\text{-}Se_2)$ (minor). Carrying out the reaction in the dark gives the latter dinuclear compound as the only observable product. This same dinuclear compound has been allowed to react with $(Ph_3P)_2Pt(PhC_2Ph)$ and $CpCo(CO)_2$ to furnish the corresponding trinuclear clusters $CpMoMnPt(PPh_3)_2(CO)_5(\mu_3\text{-}Se)_2$ and $Cp_2CoMoMn(CO)_5(\mu_3\text{-}Se)_2$. Treatment of the latter CoMoMn cluster with Me_3NO leads to the molybdenum oxo cluster $Cp_2CoMo(O)Mn(CO)_5(\mu_3\text{-}Se)_2$. The solution NMR data and the X-ray structures of all six new products are presented and fully discussed [122]. The X-ray structure of *cis*-$[\eta^2\text{-}(AuPPh_3)_2]Ph_3PCr(CO)_4\cdot THF$ has been determined and found to consist of a triangular Au_2Cr core. The observed Au–Au bond distance of 2.6937(2) Å is the shortest such distance reported for a triangular Au_2M frame [123]. The synthesis of new asymmetric heterometallic gold clusters has appeared. Good yields of $(OC)_3M(\mu\text{-}S_2CPR_3)(\mu\text{-}AuPPh_3)Mo(CO)_3$ (where M = Mn, Re; R = various alkyl groups) and $L(OC)_2Mo(\mu\text{-}S_2CPCy_3)(\mu\text{-}AuPPh_3)M'(CO)_3$ (where M′ = Mo, W; L = alkyl, NO) have been obtained from the reaction of $ClAu(PPh_3)$ with homo- or heterobinuclear anions $[(OC)_3M(\mu\text{-}S_2CPR_3)Mo(CO)_3]^-$ and $[L(OC)_2Mo(\mu\text{-}S_2CPCy_3)M'(CO)_3]^-$, respectively. The diverse polyhedral structures exhibited by these new clusters, which are fully discussed, were ascertained by X-ray crystallography [124]. New mixed-metal sulfido clusters have been synthesized and structurally characterized. The insertion of different unsaturated metal fragments into the sulfur-sulfur bond of $CpMoMn(CO)_5(\mu\text{-}S_2)$ gives rise to a variety of *closo*, *nido*, and butterfly clusters. $CpCo(CO)_2$ reacts with the MoMn dimer to furnish $Cp_2MoMnCo(CO)_5(\mu_3\text{-}S)_2$ and $Cp_2Mo(O)MnCo(CO)_3(\mu_3\text{-}S)_2$. The former product exhibits an open or *nido* MoMnCo polyhedral core with two triply bridging sulfido groups, while the latter cluster contains a closed triangular CoMnMo core with two triply bridging sulfido groups. Treatment of former MoMnCo cluster with Me_3NO gives the latter molybdenum-oxo cluster. $Fe_2(CO)_9$ and $Ru_3(CO)_{12}$ react with the starting sulfide dimer to produce $CpMoMnM(CO)_8(\mu_3\text{-}S)_2$ (where M = Fe, Ru) and $CpMoRu_3(CO)_9(\mu_3\text{-}S)_2(\mu\text{-}H)$. The X-ray structure of $CpMoMnRu(CO)_8(\mu_3\text{-}S)_2$ is shown in Fig. 12 [125].

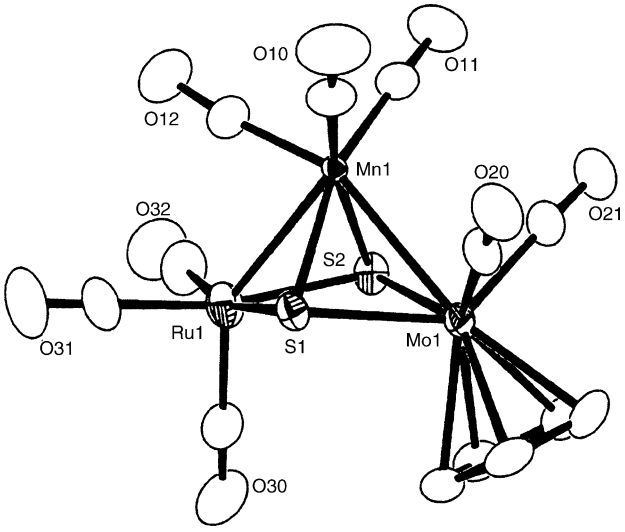

Fig. 12. X-ray structures of $CpMoMnRu(CO)_8(\mu_3\text{-}S)_2$. Reprinted with permission from Organometallics. Copyright 2003 American Chemical Society.

The complexes $CpMoMn(CO)_5(\mu\text{-}S_2)$ (where Cp = Cp, Cp^*) have been employed as starting materials for the construction of new MoMnPt and MoMnPd clusters. $(Ph_3P)_2Pt(PhC_2Ph)$ reacts with $CpMoMn(CO)_5(\mu\text{-}S_2)$ via insertion into the disulfido linkage to give $CpMoMn(CO)_5Pt(PPh_3)_2(\mu_3\text{-}S)_2$ and $Cp^*MoMn(CO)_6Pt(PPh_3)(\mu_3\text{-}S)_2$. The solid-state structure of the Cp^* derivative exhibits an *arachno* polyhedral frame with a Mo–Mn bond. Treatment of the disulfide starting compounds with $Pd(PBu^t_3)_2$ gives the trimetallic oxo clusters $CpMo(O)MnPd(PBu^t_3)(CO)_5(\mu_3\text{-}S)$, whose molecular structure was established in the case of the Cp compound [126]. Novel Au(I)-phosphido compounds have been isolated from the reaction of $ClAu(PPh_3)$ and the dinuclear compounds $[Cp(CO)_2M]_2(\mu\text{-}PH_2)(\mu\text{-}H)$ (where M = Cr, Mo). Whereas the molybdenum dimer reacts to yield the simple phosphine-substituted species $[Cp(CO)_2Mo]_2[\mu\text{-}PH(AuPPh_3)](\mu\text{-}H)$ upon deprotonation of the phosphide moiety, the reaction between $[\{Cp(CO)_2Cr\}_2(\mu\text{-}PH)(\mu\text{-}H)]^-$ and $ClAu(PPh_3)$ gives the planar Au_3Cr_3 cluster $[Cp(CO)_2Cr]_6(P_3Au_3)$. The X-ray structure of both products have been determined, and DFT calculations on the latter compound support the existence of multicenter P–Cr–Au

and multiple Cr–P bonding in this unusual cluster [127]. The heteronuclear cluster $[Cp'ReO(\mu_3\text{-}S)_2Pt_2(PPh_3)_3Cl][ReO_4]$ (where $Cp' = C_5Me_4Et$) has been isolated from the reaction between $Cp'ReCl_2S_3$ and $Pt(PPh_3)_3$ in the presence of oxygen. Included in the report are the solution spectroscopic data, X-ray diffraction structure, and cyclic voltammetric data for the $RePt_2$ cluster [128]. Deprotonation of $Mn_2(\mu\text{-}H)_2(CO)_6(\mu\text{-dppm})$ using Super-hydride yields the monoanion, followed by formation of the dianion $[Mn_2(CO)_6(\mu\text{-dppm})]^{2-}$. Treatment of these anions with $ClM(PR_3)$ (where M = Ag, R = Cy; M = Au, R = Ph, *p*-tol) affords the trinuclear compounds $Mn_2M(\mu\text{-}H)(CO)_6(\mu\text{-dppm})(PR_3)$ and the tetranuclear species $Mn_2M_2(CO)_6(\mu\text{-dppm})(PR_3)_2$. The former Mn_2M clusters are electronically deficient and readily add CO to give the electron-precise clusters $Mn_2M(\mu\text{-}H)(CO)_7(\mu\text{-dppm})(PR_3)$ [129].

The reaction of $Co_2(CO)_8$ with the pendant acetylide moiety in $Fe(CO)_4(\eta^1\text{-}PPh_2C_2Ph)$ gives the alkyne-substituted complex $(OC)_4Fe[\mu,\eta^1\text{:}\eta^2\text{-}(PPh_2CCPh)Co_2(CO)_6]$, which when allowed to react with $P(OMe)_3$ yields the cobalt-substituted compounds $(OC)_4Fe[\mu,\eta^1\text{:}\eta^2\text{-}(PPh_2CCPh)Co_2(CO)_{6-n}\{P(OMe)_3\}_n]$ (where $n = 1$, 2). Thermolysis of the mono-phosphite derivative results in P–C bond cleavage and Fe–Co bond formation to furnish the phosphido-bridged cluster $FeCo_2(CO)_6[\mu_3,\eta^2\text{-}(\perp)\text{-}CCPh][P(OMe)_3](\mu_2\text{-}PPh_2)$. Here the phenylacetylide ligand was found to perpendicularly bridge one of the Fe–Co bonds. The full details associated with the solution NMR and FAB mass spectrometry data are presented and discussed [130].

CS_2 fixation by $(CpCo)_2Fe(CO)L_2(\mu_3\text{-}S)(\mu_3\text{-}CS)$ (where L = various two-electron donor ligands) gives the cluster products $(CpCo)_2Fe(CO)L_2(\mu_3\text{-}S)(\mu_3\text{-}C_2S_3)$, which contain a capping trithiocarbonate moiety that is tethered to the Fe-C_μ edge of the trigonal bipyramidal core. The NMR behavior and cyclic voltammetric data of these new clusters are described [131]. The synthesis of $Cp^*{}_3RuIr_2(\mu_3\text{-}S)(\mu_2\text{-}SCH_2CH_2CN)_2Cl$, whose X-ray structure is shown in Fig. 13, and its reaction with alkynes, CO, and isocyanide ligands have been published. The title cluster has been isolated from the reaction of $Cp^*Ir(\mu\text{-}S)(\mu\text{-}SCH_2CH_2CN)_2Cp^*$ with $[Cp^*RuCl]_4$. Chloride replacement by CO and isocyanides gives the corresponding cationic clusters $[Cp^*{}_3RuIr_2(\mu_3\text{-}S)(\mu_2\text{-}SCH_2CH_2CN)_2L]^+$. Treatment of the starting $RuIr_2$ cluster with KPF_6 in the presence of acid gives the iminoacyl cluster $[Cp^*{}_3RuIr_2(\mu_3\text{-}S)(\mu_2\text{-}SCH_2CH_2CN)(\mu_3\text{-}SCH_2CH_2C{=}NH)]^+$ through the binding of one of the pendant nitrile groups to the Ir_2 site, followed by protonation of the coordinated nitrogen atom. The solution spectroscopic data and four X-ray structures are fully discussed [132].

New trinuclear MIr_2 and pentanuclear MIr_4 clusters containing selenido and sulfido ligands have been prepared by using $(Cp^*IrCl)_2(\mu\text{-}SeH)(\mu\text{-}SH)$ as a starting material. Some of the products that have been isolated and structurally characterized include $(Cp^*Ir)_2(MCl_2)(\mu_3\text{-}Se)_2$ (where M = Fe, Pt), $[(Cp^*Ir)_4Co(\mu_3\text{-}Se)_4]^{2+}$, and $(Cp^*Ir)_2(MCl_2)(\mu_3\text{-}Se)(\mu_3\text{-}S)$ (where M = Pd, Pt, Fe) [133]. The

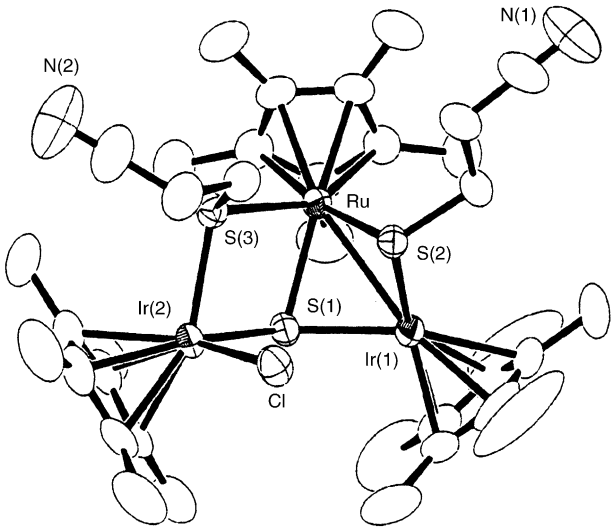

Fig. 13. X-ray structure of $Cp^*{}_3RuIr_2(\mu_3\text{-}S)(\mu_2\text{-}SCH_2CH_2CN)_2Cl$. Reprinted with permission from Organometallics. Copyright 2003 American Chemical Society.

ability of the metalloligand $Pt_2(\mu\text{-}S)_2(PPh_3)_4$ to bind π-hydrocarbon compounds of Ru(II), Os(II), Rh(III), and Ir(III) has been studied by using electrospray ionization mass spectrometry. Dicationic species of the type $[Pt_2(\mu\text{-}S)_2(PPh_3)_4ML]^{2+}$ have been observed by mass spectrometry, and the synthesis and isolation of several of the new dicationic compounds are reported [134]. The reaction of the diphosphine ligand bma with $HCCo_2NiCp(CO)_6$ has been explored. Thermolysis at 80 °C gives the zwitterionic cluster $Co_2NiCp(CO)_4(\mu\text{-}CO)[\mu_2,\eta^2,\eta^1\text{-}C(H)PPh_2C{=}C(PPh_2)C(O)OC(O)]$ as the first observable product. X-ray analysis (Fig. 14) reveals the existence of an open Co_2Ni core with the bma ligand tethered to the metallic core through phosphine attachment

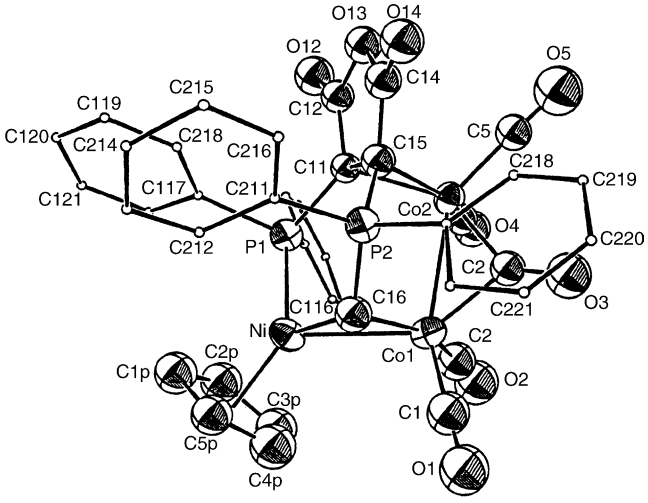

Fig. 14. X-ray structure of $Co_2NiCp(CO)_4(\mu\text{-}CO)[\mu_2,\eta^2,\eta^1\text{-}C(H)PPh_2C{=}C(PPh_2)C(O)OC(O)]$. Reprinted with permission from Organometallics. Copyright 2003 American Chemical Society.

to original μ_3-CH group and the CpNi moiety. This cluster is unstable and transforms into $Co_2NiCp(CO)_4[\mu_2,\eta^2,\sigma$-$C(H)PPh_2C{=}CC(O)OC(O)](\mu_2$-$PPh_2)$. X-ray analysis confirms the presence of a Ni–C σ bond that results from the formal coupling of the maleic anhydride ring with the CpNi moiety. The solution spectroscopic data are discussed, along with the kinetics for the P–C bond cleavage reaction and data from MO calculations that aid in the understanding of the observed cluster reactivity [135].

A report dealing with the synthesis and structural characterization of $MPtAg(\mu$-$PPh_2(C_6F_5)_2(acac)(PPh_3))$ (where M = Pt, Pd) has appeared. The structural differences found in these two clusters are outlined and discussed [136].

3.2. Tetranuclear clusters

The early-late heterometallic compound $Cp_2Ti(O^tBu)(\mu_4$-$OC)Co_3(CO)_9$ has been synthesized from $Cp_2Ti(O^tBu)$ and $Co_2(CO)_8$. The molecular structure consists of a $Co_3(CO)_9$ core with a triply bridging CO group that serves to bind the $Cp_2Ti(O^tBu)$ moiety through the oxygen atom. Mechanisms pertaining to the formation and fragmentation reactivity exhibited by this cluster are presented [137].

Photolysis of $[MeCpCr(\mu$-$SPh)]_2$ with $Fe_3(CO)_9(\mu_3$-$Se)_2$ or $Mn_2(CO)_{10}$ furnishes the new antiferromagnetic complexes $[MeCpCr(\mu$-$SPh)]_2(\mu_3$-$Se)Fe_3(CO)_9(\mu_3$-$Se)_2$, $[MeCpCr(\mu$-$SPh)]_2(\mu_3$-$Se)Mn_2(CO)_9$, and $[MeCpCr(\mu$-$SPh)]_2(\mu_4$-$Se)Mn_2(CO)_8$. The solid-state structure of each cluster has been crystallographically determined, and the role of super-exchange spin–spin interaction through the chalcogen bridge is discussed with respect to the observed magnetic properties [138]. The reactivity of the disulfido linkage in $Mn_2(CO)_7(\mu$-$S_2)$ has been investigated for its participation in small molecule activation and cluster build-up schemes. The tetranuclear cluster $CpMoMn_3(CO)_{13}(\mu_3$-$S)(\mu_4$-S) has been isolated as a minor product from the reaction of $Mn_2(CO)_7(\mu$-$S_2)$ with $Cp_2Mo_2(CO)_6$ [139]. A report describing the comparative crystallography and electrochemistry of several isostructural cubane clusters has appeared. The title clusters were prepared from the reaction of the incomplete cubane cluster $[(MeCp)_3M_3S_4]^+$ (where M = Mo, W) with group 10 alkene complexes [140]. The reaction of the metal acetylides $Cp^*M(CO)_3(CCPh)$ (where M = Mo, W) with the chalcogen-bridged cluster $Fe_3(CO)_9(\mu_3$-$S)_2$ in the presence of alkynes yields the new cluster compounds $Cp^*MFe_3(\mu_3$-$S)[\mu_3$-$C(H){=}C(R)S](CO)_6(\mu_3$-CCPh) (where R = various alkyl and aryl groups). The spectroscopic data and X-ray structures of two derivatives are presented and discussed [141]. A structural reexamination of $MoRu_3C_2(CO)_5Cp_4$ has been published. Low-temperature data collection using a CCD-equipped diffractometer have allowed for the original ambiguity in distinguishing between the Mo and Ru centers to be resolved. The revised interpretation now converges on the electron-precise cluster μ_3,η^1-$[Cp(CO)_2MoCC]Ru_3(CO)_5Cp_3$ [142]. New polynuclear clusters containing C_5 chains have been synthesized. Treatment of $BrCCo_3(CO)_7$(dppm) with $Au(C_2C_2H)(PPh_3)$ or $CpW(CO)_3(C_2C_2AuPPh_3)$ yields $[Co_3(CO)_7(dppm)]_2(\mu_3{:}\mu_3$-$CC_2C_2C)$ and $[CpW(CO)_3]C_2C_2C[Co_3(CO)_7(dppm)]$, respectively. The utility of the gold(I) derivatives in the synthesis of odd-numbered carbon chains is discussed [143]. The double-cubane cluster $[\{(Cp^*Mo)_3(\mu_3$-$S)_4Ni\}_2(\mu,\eta^2{:}\eta^2$-cod)$]^{2+}$ has been isolated from the reaction between $[(Cp^*Mo)_3(\mu_2$-$S)_3(\mu_3$-$S)]^{2+}$ and $Ni(cod)_2$. A dmad ligand reacts with the double-cubane cluster to furnish $[(Cp^*Mo)_3(\mu_3$-$S)_4Ni(\eta^2$-dmad$)]^+$. Both of these new cluster products show high catalytic activity for the intramolecular cyclization of alkynoic acids to enol lactones [144].

CO substitution in $MoIr_3(\mu_3$-$CO)_3(CO)_8Cp_2$ by isocyanides leads to varying yields of $MoIr_3(\mu_3$-$CO)_3(CO)_{8-n}L_nCp_2$ (where $L = CNBu^t$, 2,6-CNxy; $n = 1$–3). The X-ray structures of both monosubstituted clusters confirm that the isocyanide ligands are bound to iridium atoms via apical coordination. Also included in this report is the X-ray structure of $Mo_2Ir_2(\mu$-$CO)_2(CO)_8(CNBu^t)_2Cp_2$ [145]. The reaction between $MoIr_3(\mu_3$-$CO)_3(CO)_8Cp^*_2$ and PPh_3 gives the bisphosphine cluster $MoIr_3(\mu_3$-$CO)_3(CO)_6(PPh_3)_2Cp^*_2$, where the phosphine groups are shown by X-ray analysis to be coordinated to adjacent iridium atoms in the plane of the bridging CO ligands. The ligand substitution of CO by $CNBu^t$ and diphenylacetylene in $Mo_2Ir_2(\mu_3$-$CO)_3(CO)_7Cp_2$ has been described. The X-ray structural characterization of $Mo_2Ir_2(\mu_4,\eta^2$-$PhC_2Ph)(\mu_3$-$CO)_4(CO)_3(CNBu^t)Cp_2$ reveals that the adopted molecular structure exhibits a butterfly core with iridium hinge and molybdenum wingtip atoms [146]. A report dealing with the synthesis and solid-state structures, and electrochemical behavior of alkyne-coordinated Mo_2Ir_2 clusters that also contain coordinating heterocyclic bridging moieties has appeared [147]. A related paper describing the synthesis and redox activity of Mo_2Ir_2 clusters linked by phenyleneethynylene groups has been published. DFT calculations have been carried out and these data are discussed within the context of the observed cyclic voltammetry behavior [148]. The pseudooctahedral clusters $M_2Ir_2(\mu_4,\eta^2$-$RC_2R')(\mu$-$CO)_4(CO)_4(MeCp)_2$ (where M = Mo, W; R, R′ = various alkyl and aryl groups) have been synthesized from the parent $M_2Ir_2(CO)_{10}(MeCp)_2$ clusters and added alkyne. Selected derivatives were employed in the preparation of organic π-delocalized complexes where two and three separate M_2Ir_2 units have been joined by suitable phenylenevinylene linking moieties. The synthetic methodologies employed and the solution spectroscopic data on twenty-seven cluster systems are reported. Three X-ray structures accompany this paper, of which the molecular structure of $W_2Ir_2(\mu_4,\eta^2$-$MeC_2Ph)(CO)_8(MeCp)_2$ is shown in Fig. 15 [149].

New linear chain clusters containing rhenium and osmium centers have been prepared. The reaction of $Os(CO)_3(CNBu^t)_2$ with $Re_2(\mu$-$H)(\mu,\eta^1$-$C_2H_3)(CO)_8$ gives the isomeric complexes $(OC)_4(CNBu^t)ReOs(CO)_3(CNBu^t)Os(CO)_3(CNBu^t)Re(CNBu^t)(CO)_4$ and $(OC)_3(CNBu^t)_2ReOs(CO)_4Os(CO)_3(CNBu^t)Re(CNBu^t)(CO)_4$, which both con-

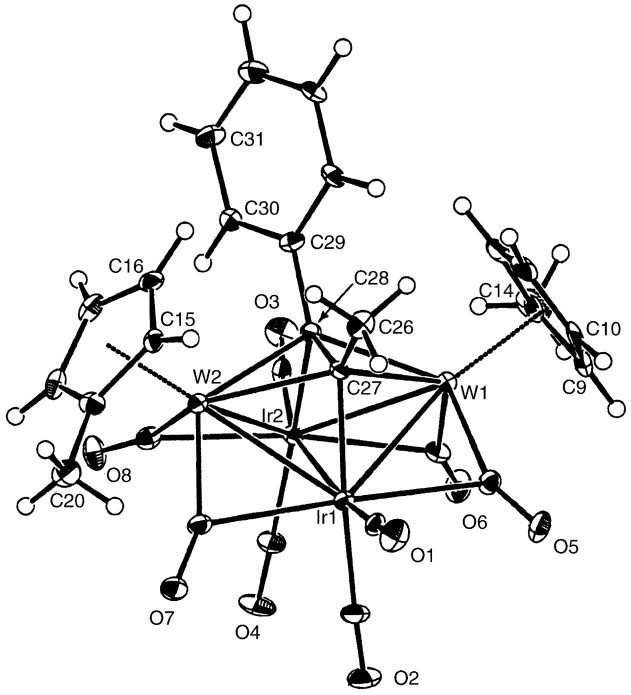

Fig. 15. X-ray structure of $W_2Ir_2(\mu_4,\eta^2\text{-}MeC_2Ph)(CO)_8(MeCp)_2$. Reprinted with permission from Organometallics. Copyright 2003 American Chemical Society.

tain a nearly linear chain of ReOsOsRe atoms based on X-ray diffraction data. The fluxional behavior of the CO ligands was explored by NMR spectroscopy, and these data have been used in a discussion pertaining to the exchange pathways available to both isomers [150]. Treatment of the carbyne compounds $[Cp(CO)_2MCPh]^+$ (where M = Mn, Re) with $[Rh(CO)_4][PPN]$ yields the tetranuclear clusters $M_2Rh_2(\mu\text{-}CPh)(\mu_3\text{-}CPh)(\mu\text{-}CO)_3(CO)_3Cp_2$, along with $Mn_3Rh_2(\mu\text{-}CPh)_2(\mu_3\text{-}CPh)(\mu\text{-}Cl)(\mu\text{-}CO)_3(CO)_2Cp_3$ and $ReRh_4(\mu_4\text{-}CPh)(\mu\text{-}CO)_4(CO)_5Cp$ which were isolated as minor side-products. The chlorine group in the former Mn_3Rh_2 cluster presumably derives from the CH_2Cl_2 solvent that was employed in the recrystallization of the cluster. The X-ray structure shown in Fig. 16 confirms the presence of this chlorine group that spans the Rh–Rh vector in this cluster [151].

Experimental evidence for direct bonding interaction between the d^{10} centers of Pd(O) and Hg(II) has been published. NMR studies reveal that the Pd center in $Hg[FeSi(OMe)_3(CO)_3(\mu\text{-}dppm)]_2Pd$ shuffles between the Hg and the two Fe groups in the linear Fe–Hg–Fe motif. The energetics associated with the observed fluxional behavior have been determined and fully discussed [152]. Electrophilic addition to the Fe_2E face of $[Fe_3(CO)_9(\mu_3\text{-}E)]^{2-}$ (where E = Se, Te) has been observed when the starting clusters are treated with $[Cp^*M(MeCN)_3]^{2+}$ (where M = Rh, Ir). The resulting tetranuclear clusters $MFe_3(\mu_4\text{-}E)(CO)_9Cp^*$ exhibit a butterfly metallic core that is ligated by the μ_4-chalcogen atom. The iridium reaction is also accompanied by the formation of the triangular clusters $IrFe_2(\mu_3\text{-}E)(CO)_7Cp^*$, whose identity was crystallographically determined in the case of the tellurium derivative [153]. The cluster $Os_3Rh(\mu\text{-}H)_3(CO)_{12}$ reacts with excess 2-vinylpyridine in refluxing $CHCl_3$ to produce $Os_4Rh(\mu\text{-}H)_4(CO)_{13}(\eta^2\text{-}NC_5H_4C_2H_2)$. The new cluster exists as a pair of isomers that differ in the configuration of the metallated vinylpyridine moiety. VT EXSY data have allowed for the accurate determination of the energetics for vinylpyridine isomerization about the cluster polyhedron. The solid-state structure of the product cluster has been solved [154]. The synthesis and molecular structure of a cluster containing a μ_4-dicarbyne moiety have been reported. Treatment of the permetallated ethene complex $(\mu_4\text{-}C{=}C)Fe_2Ru_2Cp^*_2(CO)_{10}$ with diphenylacetylene furnishes the $66e^-$ cluster $(\mu_4\text{-}C\text{-}C)Fe_2Ru_2Cp^*_2(CO)_6(\mu\text{-}PhC_2Ph)$, which contains a dimetallacyclobutariene core. This new cluster is unstable and

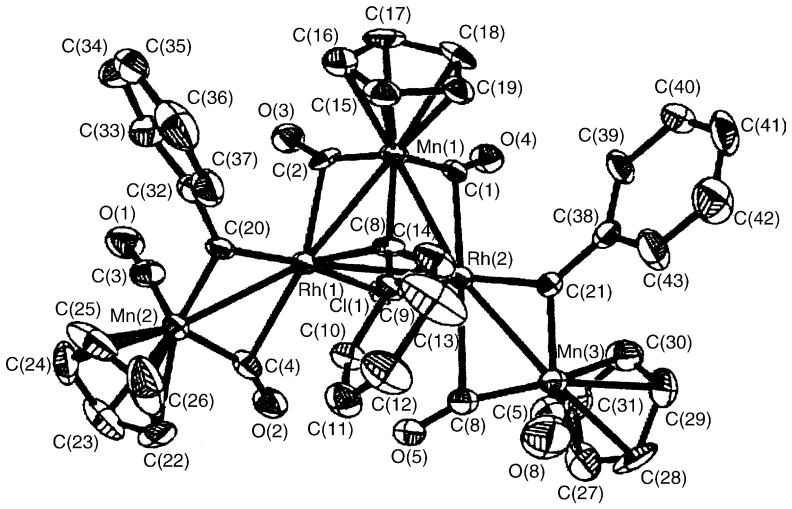

Fig. 16. X-ray structure of $Mn_3Rh_2(\mu\text{-}CPh)_2(\mu_3\text{-}CPh)(\mu\text{-}Cl)(\mu\text{-}CO)_3(CO)_2Cp_3$. Reprinted with permission from Organometallics. Copyright 2003 American Chemical Society.

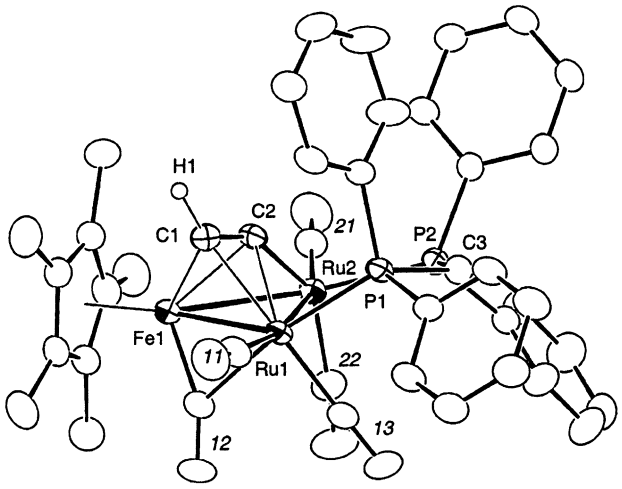

Fig. 17. X-ray structure of $(\mu_3\text{-}C_2H)FeRu_2Cp^*(CO)_5(dppm)$. Reprinted with permission from Organometallics. Copyright 2003 American Chemical Society.

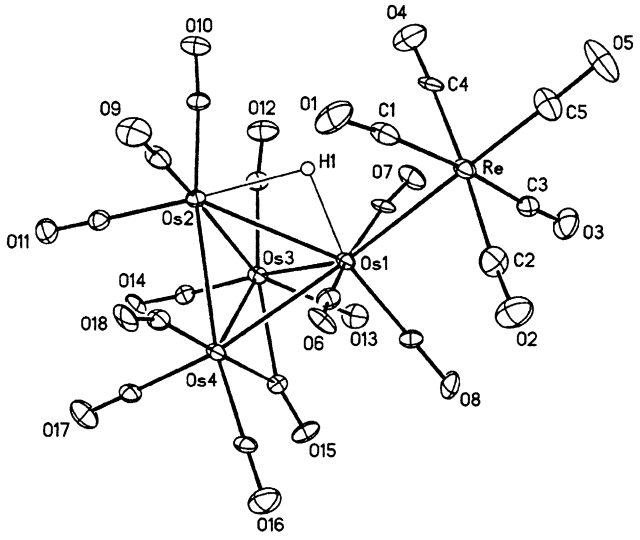

Fig. 18. X-ray structure of $ReOs_4(\mu\text{-}H)(\mu\text{-}CO)(CO)_{17}$. Reprinted with permission from Organometallics. Copyright 2003 American Chemical Society.

slowly decomposes, in part, to give an Fe_2Ru_2 compound possessing a linear 3-oxohepta-1,4-dien-6-yn-1,7-diyl skeleton [155]. Hydrogenation of the permetallated ethene ligand in $(\mu_4\text{-}C{=}C)Fe_2Ru_2Cp^*_2(CO)_8L_2$ (where $L_2 = 2CO$, dppm) has been achieved through the sequential addition of proton and hydride. α-Chloropropionic acid reacts with the decacarbonyl cluster to give the hydrido carboxylate $(\mu_4\text{-}C{=}C)(\mu\text{-}H)Fe_2Ru_2Cp^*_2(CO)_8(\mu,\kappa^1{:}\kappa^1\text{-}MeCHClCO_2)$. Reaction of the dppm-substituted derivative $(\mu_4\text{-}C{=}C)Fe_2Ru_2Cp^*_2(CO)_8(dppm)$ with Et_4NBH_4 leads to the elimination of one of the iron fragments and formation of the trinuclear acetylide cluster $(\mu_3\text{-}C_2H)FeRu_2Cp^*(CO)_5(dppm)$, whose X-ray structure is depicted in Fig. 17. The flexible coordination capability of the C_2 ligand in these clusters is discussed, as are the X-ray structures of six other cluster compounds that have been determined [156].

The synthesis and X-ray diffraction structure of $[Cp^*(PPh_3)Ir(\mu\text{-}H)_2]_2[Ag_2(OSO_2CF_3)_2]$ have been published [157]. New structural assemblies using $Pt_2(P{-}P)_2(\mu\text{-}S)_2$ are described. The heterometallic compounds $[Au_2\{Pt_2(PPh_3)_4(\mu_3\text{-}S)_2\}_2]^{2+}$, $Au_2Pt_2Cl_2(PPh_3)_4(\mu_3\text{-}S)_2$, and $Ag_2Pt_2Cl_2(dppf)_2(\mu_3\text{-}S)_2$ have been synthesized and characterized by X-ray crystallography in the case of the cationic derivative and the Ag_2Pt_4 cluster [158]. The unprecedented compound $Pt_3Hg(\mu_4\text{-}O)(\mu\text{-}OH)(\mu\text{-}Cl)Cl_3(C_6Cl_5)(PPh_3)_3$ has been isolated from the reaction of $[trans\text{-}PtCl_2(C_6Cl_5)(PPh_3)]^+$ or $[Pt(C_6Cl_5)_4]^{2+}$ with $Hg(NO_3)_2{\cdot}2H_2O$ [159].

3.3. Pentanuclear clusters

Reduction of $Fe_2(CO)_6(\mu_2\text{-}S)_2$ by Super-hydride, followed by treatment of the dianion with VCl_3, $MnCl_2$, and $CrCl_3$/Zn yields $VFe_4(CO)_{12}S_4$, $[MnFe_4(CO)_{12}S_4]^{2-}$, and $[CrFe_4(CO)_{12}S_4]^{2-}$, respectively. The details associated with the solution spectroscopic data and the molecular structures of the vanadium and manganese compounds are discussed [160]. A study dealing with the interpretation of the terminal ν(CO) spectra of various mixed-metal M_5 clusters has appeared. The IR data have been analyzed by using spherical harmonic and tensor harmonic models. The strengths and weaknesses of each method in accurately describing the ν(CO) vibrational data are outlined [161]. The reaction of $Os_4(CO)_{14}$ with $HRe(CO)_5$ has been investigated. $HRe(CO)_5$ adds to the osmium cluster at room temperature to give $ReOs_4(\mu\text{-}H)(CO)_{19}$, whose X-ray structure is shown to consist of a planar kite arrangement of metal atoms bearing an equatorially bound $Re(CO)_5$ moiety. Controlled thermolysis of this adduct at 85 °C initially affords $ReOs_4(\mu\text{-}H)(\mu\text{-}CO)(CO)_{17}$, followed by $ReOs_4(\mu\text{-}H)(CO)_{16}$. X-ray diffraction analysis of the former product (Fig. 18) reveals the presence of a distorted Os_4 tetrahedron that contains a $Re(CO)_5$ spike ligand, while the latter cluster product exhibits a trigonal bipyramidal core of metal atoms. The three X-ray structures that are presented are discussed relative to the binary clusters $Os_5(CO)_n$ (where $n = 19$, 18, 16). The fluxional behavior of the ancillary CO ligands in these three new $ReOs_4$ clusters has been studied by VT ^{13}C NMR spectroscopy, with the CO exchange mechanisms discussed [162].

3.4. Hexanuclear clusters

The activated cluster $Ru_3(CO)_{10}(MeCN)_2$ reacts with pendant alkyne linkage of $Co_3(CO)_9(\mu_3\text{-}CCO_2CH_2C_2H)$ to yield $Co_3(CO)_9[\mu_3\text{-}CCO_2CH_2CC\{HRu_3(CO)_9\}]$. X-ray diffraction analysis confirms the presence of spatially separated Co_3 and Ru_3 cluster groups that are joined by carbyne and acetylide moieties [163]. The synthesis, solution spectroscopic data, and X-ray structure of $Os_5Rh(\mu_5\text{-}C)(\mu_3\text{-}CO)(CO)_{13}Cp^*$ have been published. The $86e^-$ cluster has

been isolated in good yield from the reaction of $[Os_5(\mu_5\text{-}C)(CO)_{14}]^{2-}$ with $[Cp^*_2Rh_2]^{2+}$. The solid-state structure consists of a square-based pyramid of osmium atoms with one Os_3 face capped by the Cp^*Rh unit. An internal electronic imbalance is responsible for the adopted polyhedral structure instead of the *closo* octahedral core predicted by PSEP theory [164]. A report dealing with the synthesis and vibrational spectroscopy of $[FeNi_5(CO)_{13}]^{2-}$ has appeared. The product cluster has been obtained from the reaction of $[Ni_6(CO)_{12}]^{2-}$ with $Fe(CO)_5$ in MeCN at room temperature. The molecular structure consists of a trigonally distorted octahedron. The structural differences between the $FeNi_5$ cluster and $[Ni_6(CO)_{12}]^{2-}$ are discussed relative to the replacement of a Ni(CO) moiety by an $Fe(CO)_2$ unit. The increased steric environment in the mixed-metal system promotes facile protonation and CO-induced fragmentation reactions. One of the cluster fragmentation products isolated and structurally characterized was $[Fe_3Ni(CO)_{12}]^{2-}$ [165]. The ligand substitution chemistry in $Ru_5C(CO)_{14}Pt(cod)$ and $Ru_6C(CO)_{16}Pt(cod)$ has been explored. The cod ligand is readily replaced by CO and phosphine ligands. The former cluster reacts with CO to give $Ru_5CPt(CO)_{16}$, while the latter Ru_6Pt cluster exhibits loss of a ruthenium or Pt(cod) moiety upon reaction with added CO. Phosphine substitution at the platinum center affords $Ru_5C(CO)_{14}PtP_2$ (where $P = PPh_3$, dppm) in the case of $Ru_5C(CO)_{14}Pt(cod)$. Extrusion of the Pt(cod) moiety in the Ru_6Pt cluster by phosphines furnishes the hexaruthenium clusters $Ru_6C(CO)_{16}(PPh_3)$, $Ru_6C(CO)_{15}(PPh_3)_2$, $Ru_6C(CO)_{15}$(dppm), and $Ru_6C(CO)_{13}$(dppm)$_2$ depending upon the reaction conditions. Also isolated from the Ru_6Pt reactions in low yields were the higher nuclearity clusters $Ru_6C(CO)_{15}Pt_2$(dppm) and $Ru_6C(CO)_{16}Pt_3$(dppm)$_2$. Five X-ray structures have been determined, and mechanisms related to the substitution chemistry and ligand migration schemes are presented and discussed [166]. The synthesis and characterization of $[PtRu_5C(CO)_{15}]^{2-}$ are described. The new dianionic cluster has been obtained from $PtRu_5C(CO)_{16}$ and its reaction with KOH in methanol. The reactivity of the dianion towards $Au(PPh_3)Cl$ and platinum dihalides has also been studied as a route to higher nuclearity systems. Some of the functionalized clusters isolated and structurally characterized include $PtRu_5C(CO)_{15}(AuPPh_3)_2$, $Pt_2Ru_4C(CO)_{13}$(cod), $[Pt_3Ru_{10}C_2(CO)_{32}]^{2-}$, $Pt_4Ru_5C(CO)_{16}(PPh_3)_3$, and $Pt_2Ru_4C(CO)_{14}(PPh_3)$ [167]. The fluxional opening and closing of the platinum vertex in $PtRu_5(CO)_{15}(PBu^t_3)(\mu_{5,6}\text{-}C)$ has been demonstrated by VT NMR measurements. This cluster, which was isolated from the reaction of $Ru_5(CO)_{15}(\mu_5\text{-}C)$ with $Pt(PBu^t_3)_2$, consists of a mixture of interconverting isomers. Each isomer has been successfully recrystallized and characterized by X-ray crystallography. One isomer possesses a square pyramidal Ru_5 core that is based capped by the $Pt(PBu^t_3)$ moiety, while the second isomer is structurally similar with the $Pt(PBu^t_3)$ fragment bound to an edge of the Ru_5 square base. The NMR data allow for the calculation of both the activation and thermodynamic parameters associated with the fluxional polyhedral changes. A mechanism involving a reversible breaking and making of two Pt–Ru bonds and an oscillatory motion of the Pt moiety between the 4-fold Ru_4 site and the 2-fold edge-bridging Ru_2 site is outlined. The reaction between $Ru_5(CO)_{15}(\mu_5\text{-}C)$ and $Pd(PBu^t_3)_2$ furnishes the new clusters $PdRu_5(\mu_6\text{-}C)(CO)_{15}(PBu^t_3)$ and $Pd_2Ru_5(\mu_6\text{-}C)(CO)_{15}(PBu^t_3)_2$ as the major and minor products, respectively. The fluxional behavior exhibited by these Pd-Ru clusters has been investigated and their solid-state structures determined [168]. The ligand-substituted clusters $PtRu_5(\mu_6\text{-}C)(CO)_{15}L$ (where $L = PMe_2Ph$, PMe_3, SMe_2) and $PtRu_5(\mu_6\text{-}C)(CO)_{14}L_2$ (where $L = PMe_2Ph$, PMe_3) have been synthesized and examined for their fluxional behavior in solution. Dynamic isomerization of the ancillary L group(s) is observed and found to proceed by an intramolecular ligand exchange of the ligand between the Pt and Ru centers through bridging phosphine and sulfide intermediates. VT NMR analyses have provided the critical data related to the activation and thermodynamic parameters for each of these isomerizations. Three X-ray structures and a detailed mechanism illustrating the ligand isomerization (Fig. 19) are presented and thoroughly discussed [169].

Deprotonation of $H_4Os_4(CO)_{12}$ by Et_3N in the presence of $Au(PPh_3)Cl$ produces the new clusters $Os_4Au_2(\mu\text{-}H)_2(CO)_{11}(PPh_3)_2$, $Os_4Au_3(\mu\text{-}H)_3(CO)_{11}(PPh_3)_3$, and $Os_4Au_4(\mu\text{-}H)_2(CO)_{11}(PPh_3)_4$. Treatment of $H_4Os_4(CO)_{12}$ with Me_3NO and $Au(PPh_3)Cl$ gives $Os_4Au(\mu\text{-}H)_3(CO)_{11}(NMe_3)(PPh_3)$. The X-ray structures and electrochemical properties of these clusters are described [170]. A report dealing with the synthesis and X-ray diffraction structure of new alkynyl-Group 9/Group 11 compounds

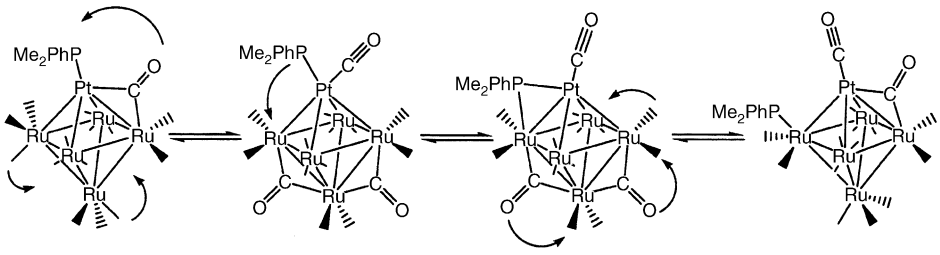

Fig. 19. Ligand exchange pathways exhibited by $PtRu_5(\mu_6\text{-}C)(CO)_{15}L$. Reprinted with permission from Inorganic Chemistry. Copyright 2003 American Chemical Society.

has appeared. The compounds presented in this report have the formula $M_2M'_4(C_2R)_8(PPh_3)_2$ (where M = Rh, Ir; M′ = Cu, Ag; R = Ph, Fc) [171]. The reaction between $[Ag_2(\mu\text{-}Ph_2PXPPh_2)_2(MeCN)_2]^{2+}$ (where X = NH, CH_2) and $[Pt(C_2C_6H_4R\text{-}p)_4]^{2-}$ (where R = H, Me) produces the luminescent hexametallic compounds $Pt_2Ag_4(\mu\text{-}Ph_2PXPPh_2)_4(C_2C_6H_4R\text{-}p)_4$ and the trinuclear complex $[PtAg_2(\mu\text{-}Ph_2PCH_2PPh_2)_2(C_2C_6H_5)_2(MeCN)_2]^{2+}$. One X-ray structure and the photophysics of these compounds are discussed [172].

3.5. Higher nuclearity clusters

The cluster compound $Os_3Rh_4(CO)_{13}(\mu_3,\eta^1{:}\eta^1\text{-}C_6H_5Me)$ has been isolated in low yield from the reaction between toluene and $Os_3Rh(CO)_{12}(\mu\text{-}H)_3$ in the presence of the hydride acceptor 4-vinylphenol. The molecular structure of this Os_3Rh_4 cluster consists of an internal Rh_4 tetrahedron with three face-capping $Os(CO)_3$ units and an unprecedented face-capping toluene ligand. A discussion of the observed product with respect to surface-bound benzenes on atomically flat closed pack surfaces possessing C_{3v} local symmetry is presented [173]. The luminescent alkynyl complexes $[Ag_6(\mu\text{-dppm})_4\{\mu_3\text{-}C_2C_2Re(N{-}N)(CO)_3\}_4]^{2+}$ (where N–N = various bipyridyl ligands) have been synthesized and their photophysical properties examined [174]. The silica-promoted synthesis of $[Ru_{10}Pt_2C_2(CO)_{28}]^{2-}$ and $Ru_5PtC(CO)_{16}$ has been achieved by using $[Ru_5C(CO)_{14}]^{2-}$ and $PtCl_2(MeCN)_2$ as starting materials. Use of the related carbide cluster $[Ru_6C(CO)_{16}]^{2-}$ furnishes $Ru_{12}PtC_2(CO)_{32}(MeCN)_2$. The molecular structure of each high-nuclearity cluster has been solved. The role of silica is believed to involve the coordination of the platinum reagent by the Si-OH surface, which yields a surface-stabilized $[Pt(MeCN)_2]^{2+}$ species that is available for the controlled addition to the ruthenium cluster [175]. Treatment of excess $[Pd(MeCN)_4]^{2+}$ with $[Os_{10}(CO)_{24}(\mu_6\text{-}C)]^{2-}$ in CH_2Cl_2 at room temperature gives $[Os_{18}Pd_3(CO)_{42}(\mu_6\text{-}C)_2]^{2-}$ in moderate yield. X-ray structural analysis reveals the presence of three metallic domains, where a triangular Pd_3 array is sandwiched between two tricapped octahedral $Os_9(CO)_{21}(\mu_6\text{-}C)$ subclusters. The ability of the $Os_{18}Pd_3$ cluster to serve as an electron reservoir without undergoing cluster fragmentation was demonstrated by cyclic voltammetry studies. The CV shows five reversible cathodic waves and two irreversible anodic processes [176].

Appendix A

bmata	2,3-bis(diphenylphosphino)maleic acid-thioanhydride
bpcd	4,5-bis(diphenylphosphino)-4-cyclopenten-1,3-dione
bppm	2,3-bis(diphenylphosphino)-*N*-phenylmaleimide
bpy	2,2′-bipyridine
cod	1,5-cyclooctadiene
cot	cyclooctatraene
Cp	cyclopentadienyl
Cp^*	pentamethylcyclopentadienyl
Cy	cyclohexyl
DMPO	5,5-dimethyl-1-pyrroline-*N*-oxide
dmad	dimethyl acetylenedicarboxylate
dmpe	1,2-bis(dimethyphosphino)ethane
dpko	bis(2-pyridyl)ketone oxime
dppa	1,2-bis(diphenylphosphino)acetylene
dppb	1,4-bis(diphenylphosphino)butane
dppe	1,2-bis(diphenylphosphino)ethane
dppef	1,2-bis(diperfluorophenylphosphino)ethane
dppf	1,1′-bis(diphenylphosphino)ferrocene
dppm	bis(diphenylphosphino)methane
dppp	1,3-bis(diphenylphosphino)propane
Fc	ferrocenyl
H_2binam	2,2′-diamino-1,1′-binaphthalene
MeCp	methylcyclopentadienyl
nbd	norbornadiene
PPN	bis(triphenylphosphine)iminium
py	pyridine
TEMPO	2,2,6,6-tetramethyl-1-piperidinyloxy
tmp	2,2,6,6-tetramethylpiperidinyl
tol	tolyl
xy	2,6-substituted xylene

References

[1] T.E. Vos, Diss. Abstr. Sect. B 63 (2003) 5240 (DA3072744).
[2] B. Qu, Abstr. Sect. B 63 (2003) 3294 (DA3059472).
[3] M.J. Abedin, Abstr. Sect. B 63 (2003) 3709 (DA3062636).
[4] W. Fu, Abstr. Sect. B 63 (2003) 3292 (DA3059440).
[5] C.E. Plečnik, Abstr. Sect. B 64 (2003) 1731 (DA3088880).
[6] O.-S. Kwon, Abstr. Sect. B 63 (2003) 3293 (DA3059452).
[7] B.K. Captain, Abstr. Sect. B 64 (2003) 200 (DA3076752).
[8] S.A. Ivanov, Abstr. Sect. B 63 (2003) 5235 (DA3072821).
[9] M.M. Hossain, H.-M. Lin, S.-G. Shyu, Organometallics 22 (2003) 3262.
[10] R.D. Adams, S. Miao, J. Organomet. Chem. 665 (2003) 43.
[11] D. Belletti, C. Graiff, C. Massera, R. Pattacini, G. Predieri, A. Tiripicchio, Inorg. Chim. Acta 356 (2003) 187.
[12] J. Guzman, B.C. Gates, J. Chem. Soc., Dalton Trans. (2003) 3303.
[13] M.A. Reynolds, I.A. Guzei, R.J. Angelici, Inorg. Chem. 42 (2003) 2191.
[14] N.E. Leadbeater, E.L. Sharp, Organometallics 22 (2003) 4167.
[15] S.F.A. Kettle, E. Boccaleri, E. Diana, R. Rossetti, P.L. Stanghellini, M.C. Iapalucci, G. Longoni, Inorg. Chem. 42 (2003) 6314.
[16] R.B. King, Inorg. Chim. Acta 350 (2003) 126.
[17] E. Lucenti, E. Cariati, C. Dragonetti, D. Roberto, J. Organomet. Chem. 669 (2003) 44.
[18] T. Kondo, F. Tsunawaki, R. Sato, Y. Ura, K. Wada, T.-A. Mitsudo, Chem. Lett. 32 (2003) 24.
[19] H.B. Ammar, J.L. Nôtre, M. Salem, M.T. Kaddachi, L. Toupet, J.-L. Renaud, C. Bruneau, P.H. Dixneuf, Eur. J. Inorg. Chem. (2003) 4055.
[20] H. Zhang, C.-B. Yang, Y.-Y. Li, Z.-R. Donga, J.-X. Gao, H. Nakamura, K. Murata, T. Ikariya, Chem. Commun. (2003) 142.

[21] A.P. Meacham, K.L. Druce, Z.R. Bell, M.D. Ward, J.B. Keister, A.B.P. Lever, Inorg. Chem. 42 (2003) 7887.
[22] M. Haukka, P. Da Costa, S. Luukkanen, Organometallics 22 (2003) 5137.
[23] A. Chehata, A. Oviedo, A. Arévalo, S. Bernés, J.J. García, Organometallics 22 (2003) 1585.
[24] C. Alvarez-Toledano, E. Delgado, B. Donnadieu, E. Hernández, G. Martín, F. Zamora, Inorg. Chim. Acta 351 (2003) 119.
[25] I.-C. Hwang, K. Seppelt, Inorg. Chem. 42 (2003) 7116.
[26] J.S.-Y. Wong, Z.-Y. Lin, W.-T. Wong, Inorg. Chem. Commun. 6 (2003) 713.
[27] R.D. Adams, B. Captain, J.L. Smith Jr., J. Organomet. Chem. 683 (2003) 421.
[28] W.-Y. Yeh, Y.-C. Liu, S.-M. Peng, G.-H. Lee, Organometallics 22 (2003) 2361.
[29] L. Vieille-Petit, B. Therrien, G. Süss-Fink, Inorg. Chim. Acta 355 (2003) 394.
[30] L. Vieille-Petit, B. Therrien, G. Süss-Fink, Eur. J. Inorg. Chem. (2003) 3707.
[31] M. Abe, T. Michi, A. Sato, T. Kondo, W. Zhou, S. Ye, K. Uosaki, Y. Sasaki, Angew. Chem. Int. Ed. 42 (2003) 2912.
[32] L. Vieille-Petit, S. Unternährer, B. Therrien, G. Süss-Fink, Inorg. Chim. Acta 355 (2003) 335.
[33] J.A. Cabeza, I. da Silva, I. del Río, S. García-Granda, V. Riera, Inorg. Chim. Acta 347 (2003) 107.
[34] G. Gervasio, D. Marabello, P.J. King, E. Sappa, A. Secco, J. Organomet. Chem. 671 (2003) 137.
[35] L.P. Clarke, J.E. Davies, D.V. Krupenya, P.R. Raithby, G.P. Shields, G.L. Starova, S.P. Tunik, J. Organomet. Chem. 683 (2003) 313.
[36] Q. Lin, W.K. Leong, Organometallics 22 (2003) 639.
[37] S.P. Tunik, V.D. Khripoun, I.A. Balova, M.E. Borovitov, I.N. Domnin, E. Nordlander, M. Haukka, T.A. Pakkanen, D.H. Farrar, Organometallics 22 (2003) 3455.
[38] M. Ohashi, K. Matsubara, T. Iizuka, H. Suzuki, Angew. Chem. Int. Ed. 42 (2003) 937.
[39] A. Inagaki, D.G. Musaev, T. Toshifumi, H. Suzuki, K. Morokuma, Organometallics 22 (2003) 1718.
[40] T. Takao, A. Inagaki, E. Murotani, T. Imamura, H. Suzuki, Organometallics 22 (2003) 1361.
[41] M. Akther, K.A. Azam, S.M. Azad, S.E. Kabir, K.M.A. Malik, R. Mann, Polyhedron 22 (2003) 355.
[42] Y. Nakajima, H. Suzuki, Organometallics 22 (2003) 959.
[43] J.A. Cabeza, I. del Río, V. Riera, M. Suárez, C. Álvarez-Rúa, S. García-Granda, S.H. Chuang, J.R. Hwu, Eur. J. Inorg. Chem. (2003) 4159.
[44] F.W. Vergeer, M.J. Calhorda, P. Matousek, M. Towrie, F. Hartl, J. Chem. Soc., Dalton Trans. (2003) 4084.
[45] W.H. Watson, M.A. Mendez-Rojas, Y. Zhao, M.G. Richmond, J. Chem. Crystallogr. 33 (2003) 765.
[46] E. Rosenberg, F. Spada, K. Sugden, B. Martin, L. Milone, R. Gobetto, A. Viale, J. Fiedler, J. Organomet. Chem. 668 (2003) 51.
[47] L. D'Ornelas, T. Castrillo, L. de, B. Hernández, A. Narayan, R. Atencio, Inorg. Chim. Acta 342 (2003) 1.
[48] K.M. Hanif, M.S. Islam, S.E. Kabir, K.M.A. Malik, M.A. Miah, N. Wakelin, J. Chem. Crystallogr. 33 (2003) 859.
[49] J.A. Cabeza, I. del Río, P. García-Álvarez, V. Riera, M. Suárez, S. García-Granda, J. Chem. Soc., Dalton Trans. (2003) 2808.
[50] J.A. Cabeza, I. del Río, S. García-Granda, L. Martínez-Méndez, M. Moreno, V. Riera, Organometallics 22 (2003) 1164.
[51] J.A. Cabeza, I. da Silva, I. del Río, S. García-Granda, V. Riera, M.G. Sánchez-Vega, Organometallics 22 (2003) 1519.
[52] D. Belletti, C. Graiff, V. Lostao, R. Pattacini, G. Predieri, A. Tiripicchio, Inorg. Chim. Acta 347 (2003) 137.
[53] D. Belletti, C. Graiff, C. Massera, A. Minarelli, G. Predieri, A. Tiripicchio, D. Acquotti, Inorg. Chem. 42 (2003) 8509.
[54] C. Babij, H. Chen, L. Chen, A.J. Pöe, J. Chem. Soc., Dalton Trans. (2003) 3184.
[55] K. Ejsmont, W.H. Watson, J. Liu, M.G. Richmond, J. Chem. Crystallogr. 33 (2003) 541.
[56] G.M.G. Hossain, M.I. Hyder, S.E. Kabir, K.M.A. Malik, M.A. Miah, T.A. Siddiquee, Polyhedron 22 (2003) 633.
[57] K. Raghuraman, S.S. Krishnamurthy, M. Nethaji, J. Organomet. Chem. 669 (2003) 79.
[58] A.R. O'Connor, C. Nataro, A.L. Rheingold, J. Organomet. Chem. 679 (2003) 72.
[59] S.G. Bott, H. Shen, R.A. Senter, M.G. Richmond, Organometallics 22 (2003) 1953.
[60] S.N. Konchenko, N.A. Pushkarevsky, A.V. Virovets, M. Scheer, J. Chem. Soc., Dalton Trans. (2003) 581.
[61] C. Graiff, G. Predieri, A. Tiripicchio, Eur. J. Inorg. Chem. (2003) 1659.
[62] I.Y. Guzman-Jimenez, J.W. van Hal, K.H. Whitmire, Organometallics 22 (2003) 1914.
[63] Y.-F. Tzeng, C.-Y. Wu, W.-S. Hwang, C.-H. Hung, J. Organomet. Chem. 687 (2003) 16.
[64] M.G. Ballinas-López, M.J. Rosales-Hoz, E.V. García-Báez, Inorg. Chem. Commun. 6 (2003) 675.
[65] M.G. Ballinas-López, E.V. García-Báez, M.J. Rosales-Hoz, Polyhedron 22 (2003) 3403.
[66] D.P. Klein, M.V. Ovchinnikov, A. Ellern, R.J. Angelici, Organometallics 22 (2003) 3691.
[67] A.J. Edwards, J. Lewis, C.-K. Li, C.A. Morewood, P.R. Raithby, G.P. Shields, Inorg. Chem. Commun. 6 (2003) 1291.
[68] N.S. Lokbani-Azzouz, A. Boucekkine, J.-F. Halet, J.-Y. Saillard, J. Clust. Sci. 14 (2003) 49.
[69] R. Gautier, F. Chédéric, G. Süss-Fink, J.-Y. Saillard, Inorg. Chem. 42 (2003) 8278.
[70] Y. Li, W.-T. Wong, J. Chem. Soc., Dalton Trans. (2003) 398.
[71] Y. Li, W.-T. Wong, Z.-Y. Lin, Organometallics 22 (2003) 1029.
[72] W.-Y. Wong, F.-L. Ting, Z. Lin, Organometallics 22 (2003) 5100.
[73] R.D. Adams, B. Captain, W. Fu, Inorg. Chem. 42 (2003) 1328.
[74] C.M.G. Judkins, K.A. Knights, B.F.G. Johnson, Y.R. de Miguel, Polyhedron 22 (2003) 3.
[75] Y. Ohki, N. Uehara, H. Suzuki, Organometallics 22 (2003) 59.
[76] P.J. Dyson, J.S. McIndoe, Inorg. Chim. Acta 354 (2003) 68.
[77] J.S.-Y. Wong, Z.-Y. Lin, W.-T. Wong, Organometallics 22 (2003) 4798.
[78] T. Beringhelli, E. Cariati, C. Dragonetti, S. Galli, E. Lucenti, D. Roberto, A. Sironi, R. Ugo, Inorg. Chim. Acta 354 (2003) 79.
[79] N.L. Cromhout, A.R. Manning, A.J. Palmer, C.J. McAdam, B.H. Robinson, J. Simpson, Inorg. Chim. Acta 354 (2003) 54.
[80] J.D. King, M.J. Mays, M. McPartlin, G.A. Solan, C.L. Stone, J. Organomet. Chem. 681 (2003) 102.
[81] F.-E. Hong, C.-P. Chang, H. Chang, Y.-L. Huang, Y.-C. Chang, J. Organomet. Chem. 677 (2003) 80.
[82] J.M. O'Connor, K.D. Bunker, J. Organomet. Chem. 671 (2003) 1.
[83] M.I. Bruce, M.E. Smith, N.N. Zaitseva, B.W. Skelton, A.H. White, J. Organomet. Chem. 670 (2003) 170.
[84] G.J. Harfoot, B.K. Nicholson, J. Organomet. Chem. 669 (2003) 106.
[85] A. Shinozaki, H. Seino, M. Hidai, Y. Mizobe, Organometallics 22 (2003) 4636.
[86] S.G. Bott, T. Muňoz Jr., M.G. Richmond, J. Chem. Crystallogr. 33 (2003) 549.
[87] M. Ebihara, M. Iiba, S. Higashi, N. Tsuzuki, T. Kawamura, T. Morioka, S. Ozawa, T. Yamabe, H. Masuda, Polyhedron 22 (2003) 3413.
[88] J.H. Kaldis, P. Morawietz, M.J. McGlinchey, Organometallics 22 (2003) 1293.
[89] K.A. Bunten, D.H. Farrar, A.J. Pöe, Organometallics 22 (2003) 3448.
[90] C. Li, E. Widjaja, M. Garland, J. Am. Chem. Soc. 125 (2003) 5540.
[91] M. Finger, J. Reinhold, Inorg. Chem. 42 (2003) 8128.

[92] K. Besancon, T. Lumini, G. Laurenczy, S. Detti, K. Schenk, R. Roulet, J. Chem. Soc., Dalton Trans. (2003) 968.
[93] L. Garlaschelli, F. Greco, G. Peli, M. Manassero, M. Sansoni, R.D. Pergola, J. Chem. Soc., Dalton Trans. (2003) 4700.
[94] J. Sánchez-Nieves, B.T. Sterenberg, K.A. Udachin, A.J. Carty, Can. J. Chem. 81 (2003) 1149.
[95] C. Evans, B.K. Nicholson, J. Organomet. Chem. 665 (2003) 95.
[96] L. Garlaschelli, F. Greco, G. Peli, M. Manassero, M. Sansoni, R. Gobetto, L. Salassa, R.D. Pergola, Eur. J. Inorg. Chem. (2003) 2108.
[97] A. Choualeb, P. Braunstein, J. Rosé, S.-E. Bouaoud, R. Welter, Organometallics 22 (2003) 4405.
[98] B.E. Ali, J. Mol. Catal. A 203 (2003) 53.
[99] T. Akioka, Y. Inoue, A. Yanagawa, M. Hiyamizu, Y. Takagi, A. Sugimori, J. Mol. Catal. A 202 (2003) 31.
[100] C. Tejel, M.A. Ciriano, B.E. Villarroya, J.A. López, F.J. Lahoz, L.A. Oro, Angew. Chem. Int. Ed. 42 (2003) 530.
[101] D.H. Farrar, E.V. Grachova, M. Haukka, B.T. Heaton, J.A. Iggo, T.A. Pakkanen, I.S. Podkorytov, S.P. Tunik, Inorg. Chim. Acta 354 (2003) 11.
[102] E.V. Grachova, M. Haukka, B.T. Heaton, E. Nordlander, T.A. Pakkanen, I.S. Podkorytov, S.P. Tunik, J. Chem. Soc., Dalton Trans. (2003) 2468.
[103] S.P. Tunik, I.O. Koshevoy, A.J. Pöe, D.H. Farrar, E. Nordlander, M. Haukka, T.A. Pakkanen, J. Chem. Soc., Dalton Trans. (2003) 2457.
[104] C.S. Hong, L.A. Berben, J.R. Long, J. Chem. Soc., Dalton Trans. (2003) 2119.
[105] R.D. Pergola, E. Comensoli, L. Garlaschelli, M. Manassero, M. Sansoni, D. Strumolo, Eur. J. Inorg. Chem. (2003) 213.
[106] A. Albinati, P. Leoni, L. Marchetti, S. Rizzato, Angew. Chem. Int. Ed. 42 (2003) 5990.
[107] D. Brevet, Y. Mugnier, F. Lemaître, D. Lucas, S. Samreth, P.D. Harvey, Inorg. Chem. 42 (2003) 4909.
[108] F. Lemaître, D. Lucas, K. Groison, P. Richard, Y. Mugnier, P.D. Harvey, J. Am. Chem. Soc. 125 (2003) 5511.
[109] E. Alonso, J. Forniés, C. Fortuño, A. Martín, A.G. Orpen, Organometallics 22 (2003) 2723.
[110] T. Murahashi, T. Uemura, H. Kurosawa, J. Am. Chem. Soc. 125 (2003) 8436.
[111] P. Leoni, F. Marchetti, L. Marchelli, M. Pasquali, Chem. Commun. (2003) 2372.
[112] E.G. Mednikov, L.F. Dahl, J. Chem. Soc., Dalton Trans. (2003) 3117.
[113] H. Paul, S. Bhaduri, G.K. Lahiri, Organometallics 22 (2003) 3019.
[114] E.G. Mednikov, S.A. Ivanov, J. Wittayakun, L.F. Dahl, J. Chem. Soc., Dalton Trans. (2003) 1686.
[115] E.G. Mednikov, S.A. Ivanov, L.F. Dahl, Angew. Chem. Int. Ed. 42 (2003) 323.
[116] A. Sundararaman, R.A. Lalancette, L.N. Zakharov, A.L. Rheingold, F. Jäkle, Organometallics 22 (2003) 3526.
[117] J.C. Garrison, R.S. Simons, C.A. Tessier, W.J. Youngs, J. Organomet. Chem. 673 (2003) 1.
[118] M.A. Casado, J.J. Pérez-Torrente, M.A. Ciriano, I.T. Dobrinovitch, F.J. Lahoz, L.A. Oro, Inorg. Chem. 42 (2003) 3956.
[119] M. Shieh, R.-L. Chung, C.-H. Yu, M.-H. Hsu, C.-H. Ho, S.-M. Peng, Y.-H. Liu, Inorg. Chem. 42 (2003) 5477.
[120] B. Ahrens, J.M. Cole, J.P. Hickey, J.N. Martin, M.J. Mays, P.R. Raithby, S.J. Teat, A.D. Woods, J. Chem. Soc., Dalton Trans. (2003) 1389.
[121] N. Auvray, P. Braunstein, S. Mathur, M. Veith, H. Shen, S. Hüfner, New. J. Chem. 27 (2003) 155.
[122] R.D. Adams, O.-S. Kwon, Inorg. Chem. 42 (2003) 6175.
[123] M.W. Esterhuysen, H.G. Raubenheimer, Acta Crystallogr. Sec. C 59 (2003) 286.
[124] M. Wang, D. Miguel, E.M. López, J. Pérez, V. Riera, C. Bois, Y. Jeannin, J. Chem. Soc., Dalton Trans. (2003) 961.
[125] R.D. Adams, S. Miao, Organometallics 22 (2003) 2492.
[126] R.D. Adams, O.-S. Kwon, J. Clust. Sci. 14 (2003) 367.
[127] U. Vogel, P. Sekar, R. Ahlrichs, U. Huniar, M. Scheer, Eur. J. Inorg. Chem. (2003) 1518.
[128] S.H. Pawlicki, B.C. Noll, M.R. Dubois, J. Coord. Chem. 56 (2003) 41.
[129] X.-Y. Liu, V. Riera, M.A. Ruiz, M. Lanfranchi, A. Tiripicchio, Organometallics 22 (2003) 4500.
[130] M.J. Mays, K. Sarveswaran, G.A. Solan, Inorg. Chim. Acta 354 (2003) 21.
[131] A.R. Manning, C.J. McAdam, A.J. Palmer, B.H. Robinson, J. Simpson, J. Chem. Soc., Dalton Trans. (2003) 4472.
[132] F. Takagi, H. Seino, M. Hidai, Y. Mizobe, Organometallics 22 (2003) 1065.
[133] S. Nagao, H. Seino, M. Hidai, Y. Mizobe, J. Organomet. Chem. 669 (2003) 124.
[134] S.-W.A. Fong, T.S.A. Hor, W. Henderson, B.K. Nicholson, S. Gardyne, S.M. Devoy, J. Organomet. Chem. 679 (2003) 24.
[135] S.G. Bott, K. Yang, K.A. Talafuse, M.G. Richmond, Organometallics 22 (2003) 1383.
[136] E. Alonso, J. Forniés, C. Fortuño, A. Martín, A.G. Orpen, Organometallics 22 (2003) 5011.
[137] S. Niibayashi, K. Mitsui, K. Matsubara, H. Nagashima, Organometallics 22 (2003) 4885.
[138] A.A. Pasynskii, I.V. Skabitski, Y.V. Torubaev, N.I. Semenova, V.M. Novotortsev, O.G. Ellert, K.A. Lyssenko, J. Organomet. Chem. 671 (2003) 91.
[139] R.D. Adams, B. Captain, O.-S. Kwon, S. Miao, Inorg. Chem. 42 (2003) 3356.
[140] K. Herbst, P. Zanello, M. Corsini, N. D'Amelio, L. Dahlenburg, M. Brorson, Inorg. Chem. 42 (2003) 974.
[141] P. Mathur, A.K. Bhunia, C. Srinivasu, S.M. Mobin, J. Organomet. Chem. 670 (2003) 144.
[142] C.S. Griffith, G.A. Koutsantonis, B.W. Skelton, A.H. White, J. Organomet. Chem. 672 (2003) 17.
[143] M.I. Bruce, B.W. Skelton, A.H. White, N.N. Zaitseva, J. Organomet. Chem. 683 (2003) 398.
[144] I. Takei, Y. Wakebe, K. Suzuki, Y. Enta, T. Suzuki, Y. Mizobe, M. Hidai, Organometallics 22 (2003) 4639.
[145] A.J. Usher, M.G. Humphrey, A.C. Willis, J. Organomet. Chem. 678 (2003) 72.
[146] A.J. Usher, M.G. Humphrey, A.C. Willis, J. Organomet. Chem. 682 (2003) 41.
[147] E.G.A. Notaras, N.T. Lucas, M.G. Humphrey, A.C. Willis, A.D. Rae, Organometallics 22 (2003) 3659.
[148] N.T. Lucas, E.G.A. Notaras, S. Petrie, R. Stranger, M.G. Humphrey, Organometallics 22 (2003) 708.
[149] N.T. Lucas, E.G.A. Notaras, M.P. Cifuentes, M.G. Humphrey, Organometallics 22 (2003) 284.
[150] R. Dhawan, F. Jiang, G.P.A. Yap, R.K. Pomeroy, J. Clust. Sci. 14 (2003) 9.
[151] L. Zhang, B. Zhu, N. Xiao, Q. Xu, N. Tsumori, J. Sun, Y. Yin, J. Chen, Organometallics 22 (2003) 4369.
[152] W. Schuh, P. Braunstein, M. Bénard, M.-M. Rohmer, R. Welter, Angew. Chem. Int. Ed. 42 (2003) 2161.
[153] S.N. Konchenko, N.A. Pushkarevsky, M. Scheer, J. Clust. Sci. 14 (2003) 299.
[154] J.P.-K. Lau, W.-T. Wong, Inorg. Chem. Commun. 6 (2003) 174.
[155] M. Terada, G. Higashihara, A. Inagaki, M. Akita, Chem. Commun. (2003) 2984.
[156] M. Terada, M. Akita, Organometallics 22 (2003) 355.
[157] M. Gorol, N.C. Mösch-Zanetti, H.W. Roesky, M. Noltemeyer, H.-G. Schmidt, Chem. Commun. (2003) 46.
[158] Z. Li, K.F. Mok, T.S.A. Hor, J. Organomet. Chem. 682 (2003) 73.
[159] I. Ara, J. Forniés, L. Gabilondo, M.A. Usón, Inorg. Chim. Acta 347 (2003) 155.

[160] B. Zhuang, J. Chen, L. He, H. Sun, Z. Zhou, C. Lin, K. Wu, Z. Huang, J. Organomet. Chem. 682 (2003) 59.
[161] S.F.A. Kettle, E. Diana, R. Rossetti, R.D. Pergola, E. Boccaleri, P.L. Stanghellini, Inorg. Chim. Acta 350 (2003) 32.
[162] J.P. Canal, G.P.A. Yap, R.K. Pomeroy, Organometallics 22 (2003) 3439.
[163] W.H. Watson, J.-C. Wang, M.G. Richmond, J. Chem. Crystallogr. 33 (2003) 957.
[164] J.P.-K. Lau, W.-T. Wong, Inorg. Chem. Commun. 6 (2003) 733.
[165] R.D. Pergola, E. Diana, L. Garlaschelli, G. Peli, M. Manassero, M. Sansoni, D. Strumolo, Inorg. Chim. Acta 350 (2003) 107.
[166] S. Hermans, T. Khimyak, N. Feeder, S.J. Teat, B.F.G. Johnson, J. Chem. Soc., Dalton Trans. (2003) 672.
[167] T. Khimyak, B.F.G. Johnson, S. Hermans, A.D. Bond, J. Chem. Soc., Dalton Trans. (2003) 2651.
[168] R.D. Adams, B. Captain, W. Fu, P.J. Pellechia, M.D. Smith, Inorg. Chem. 42 (2003) 2094.
[169] R.D. Adams, B. Captain, W. Fu, P.J. Pellechia, Inorg. Chem. 42 (2003) 3111.
[170] Y. Li, W.-T. Wong, Eur. J. Inorg. Chem. (2003) 2651.
[171] M.I. Bruce, N.N. Zaitseva, B.W. Skelton, N. Somers, A.H. White, Aust. J. Chem. 56 (2003) 509.
[172] Q.-H. Wei, G.-Q. Yin, Z. Ma, L.-X. Shi, Z.-N. Chen, Chem. Commun. (2003) 2188.
[173] J.P.-K. Lau, Z.-Y. Lin, W.-T. Wong, Angew. Chem. Int. Ed. 42 (2003) 1935.
[174] V.W.-W. Yam, W.-Y. Lo, N. Zhu, Chem. Commun. (2003) 2446.
[175] B.F.G. Johnson, S. Hermans, T. Khimyak, Eur. J. Inorg. Chem. (2003) 1325.
[176] K.-F. Yung, W.-T. Wong, Angew. Chem. Int. Ed. 42 (2003) 553.